Aalborg Universitet

AALBORG UNIVERSITY

Small-Scale CCHP Systems for Waste Heat Recovery from Cement Plants: Thermodynamic, Sustainability and Economic Implications

Nami, Hossein; Anvari-Moghaddam, Amjad

Published in:
Energy

DOI (link to publication from Publisher):
10.1016/j.energy.2019.116634

Creative Commons License
CC BY-NC-ND 4.0

Publication date:
2020

Document Version
Accepted author manuscript, peer reviewed version

Link to publication from Aalborg University

Citation for published version (APA):
Nami, H., & Anvari-Moghaddam, A. (2020). Small-Scale CCHP Systems for Waste Heat Recovery from Cement Plants: Thermodynamic, Sustainability and Economic Implications. *Energy*, *192*, Article 116634. https://doi.org/10.1016/j.energy.2019.116634

General rights
Copyright and moral rights for the publications made accessible in the public portal are retained by the authors and/or other copyright owners and it is a condition of accessing publications that users recognise and abide by the legal requirements associated with these rights.

- Users may download and print one copy of any publication from the public portal for the purpose of private study or research.
- You may not further distribute the material or use it for any profit-making activity or commercial gain
- You may freely distribute the URL identifying the publication in the public portal -

Take down policy
If you believe that this document breaches copyright please contact us at vbn@aub.aau.dk providing details, and we will remove access to the work immediately and investigate your claim.

Downloaded from vbn.aau.dk on: December 04, 2025

Small-Scale CCHP Systems for Waste Heat Recovery from Cement Plants: Thermodynamic, Sustainability and Economic Implications

Hossein Nami, Amjad Anvari-Moghaddam*

Department of Energy Technology, Aalborg University, Aalborg, Denmark

Postal Adresse: Pontoppidantræde 111, DK-9220 Aalborg East, Denmark

Emails:

hona@et.aau.dk

*aam@et.aau.dk (Corresponding author, Tel: +45-71312083)

Abstract

In this paper, different combined cooling, heating and power (CCHP) systems are introduced and studied for waste heat recovery from a cement plant located in Şanliurfa, Turkey considering domestic applications. One of the systems is based on the steam Rankine cycle and the next is based on recuperative organic Rankine cycle (ORC), while both of them are equipped with a LiBr-H2O absorption chiller to produce cooling. Different working fluids are considered in the ORC simulation. Energy, exergy and exergoeconomic principles are applied to compare the examined systems from thermodynamic, sustainability and economic aspects. It is observed that utilizing siloxanes as the working fluid leads to efficient performance of the ORC. Besides, employed heat recovery steam generator in the Rankine cycle and evaporator in the ORC found to be the most exergy destructive components. Results revealed that the CCHP system operating with ORC (MM as working fluid) has a better performance thermodynamically with energy utilization factor, exergy efficiency and sustainability index of 98.07, 63.6% and 2.747, respectively. This is while, Rankine-based CCHP is economically preferable with a payback period of 4.738 year compared to the system operating with ORC and a payback period of 5.074 year.

Keywords: Waste heat recovery, Organic Rankine cycle (ORC), Domestic heating/cooling, Exergoeconomic, Payback period, Sustainability.

Graphical abstract:

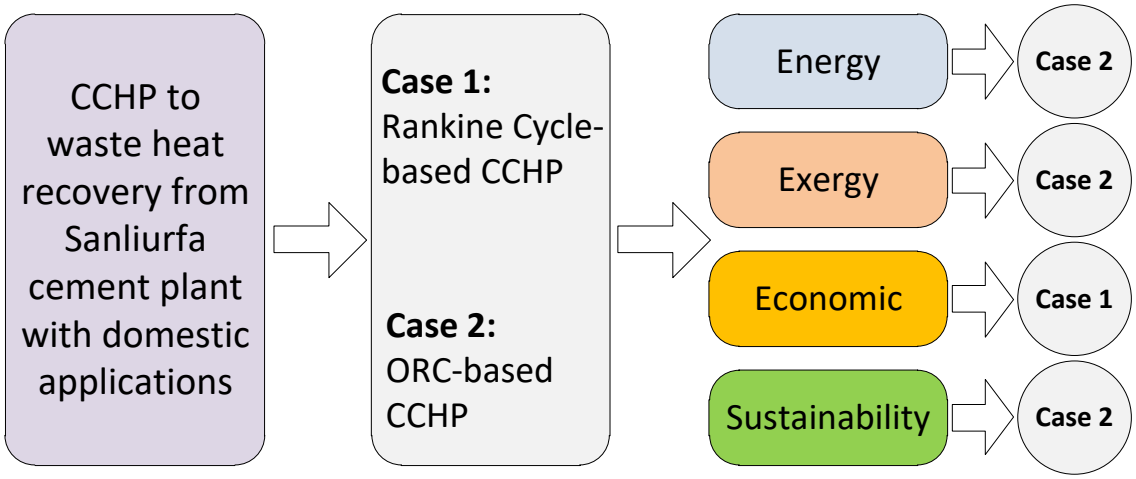

Nomenclature

Abbreviations

A	heat transfer area
Abs	absorber
Cond	condenser
CRF	capital recovery factor
EE	exergy efficiency
Eva	evaporator
Gen	generator
HE	heat exchanger
HRSG	heat recovery steam generator
HW	hot water
IHE	internal heat exchanger
NPP	net produced power
ORC	organic Rankine cycle
ORCC	ORC unit condenser
ORCE	ORC unit evaporator
ORCP	ORC unit pump
ORCT	ORC unit turbine
P	pump
SC	steam condenser
SHE	solution heat exchanger
SPC	space cooling
SPH	space heating
SP	pump utilized in steam cycle
ST	steam turbine

Latin letters

e	specific physical exergy (kJ/kg)
$\dot{E}$	exergy flow rate (kW)
h	specific enthalpy (J/kg)
$\dot{m}$	mass flow rate (kg/s)
$\dot{Q}$	heat transfer rate (kW)
R	gas constant (kJ/kg K)
s	entropy (kJ/kg K)
T	temperature (K)
$\dot{W}$	power (kW)
Z	component investment cost ($)
$\dot{Z}$	component investment cost rate ($/s)

Greek letters

η	energy efficiency (-)
η_{gen}	electric generator efficiency
ε	exergy efficiency (-)

Subscripts

ch	chemical
D	destruction
e	outlet
eco	economizer
eva	evaporator
g	gas
i	inlet
is	isentropic
LMTD	logarithmic mean temperature difference
ph	physical
s	steam
t	overall
0	ambient conditions

1. Introduction

The cement industry is one of the most energy intensive sectors which wastes almost around 40% of overall input energy. This is while the cement plants are one of the top two main industries emitting greenhouse gasses [1,2]. Typically 75% of the total energy consumption in the cement sectors is thermal energy and the rest is electrical energy [3]. On the other hand, there is a growing need to cement in the developing countries. Yearly cement production capacity in 1950 was 150 million tons, while it has reached the value of 3.6 billion tons in 2012 which clarifies that more attention should be paid to this sector from the energy consumption point of view. Large values of waste heat in this industry attracts researchers' attention to provide different techniques of energy harvesting. Following literature review represents some of the most recent findings in this scientific area.

Energy audit for pyro-processing unit of a cement plant in Iran and a feasibility study of waste heat harvesting was studied by Ghalandari et al. [4]. They showed that clinker formation consumes almost half of the total input energy and the rest is lost in different forms like radiation and pyro-processing exhaust gases. The obtained thermodynamic and economic results also revealed that about 5.2 MWh power can be produced via waste heat recovery from the grate cooler and exhaust gases with a payback period of 6.7 years. Júnior et al. [5] investigated employing Kalina cycle to waste heat recovery from Brazilian cement industry with a daily production capacity of 2100 tons clinker. In the same study, the effects of a change in ammonia concentration and pinch point temperature difference on the system thermodynamic and economic performances were obtained. In addition, they considered the net output power as the objective function of the optimization procedure. It was found that the electricity generation could reach the value of 2430 kW, while the energy and exergy efficiencies could be around 23 and 48%, respectively. Mohammadi et al. [6] considered both low- and high-temperature waste sources of cement plant as a potential for electricity generation and compared different bottom cycles as the energy harvesting system. They showed that in the case of high-temperature sources, recuperative ORC is the best option and has the capability of generating almost 7 MW power from waste heat recovery of a plant with a capacity of 3400 tons per day. Also, they reported that in the case of low-temperature sources simple ORC performs better than the supercritical CO_2 cycle. Authors of [7] considered a Norwegian cement plant with a capacity of about 1.3 million tons per year as a case study for waste heat recovery from kiln exhaust gas. In that study, waste heat was utilized for low-pressure steam and hot water production. Based on the results provided in their study, 6 MW hot water and 20 MW

low-pressure steam can be generated when no raw meal is produced. Han et al. [8] proposed a simple steam power cycle with the aim of waste heat harvesting from cement plant and optimized the combined system, including bottoming power generating system and the base cement plant, using the pinch and exergy analysis. The case study was a cement plant in Northwest China with clinker production line of 2500 tons per day. Power generation capacity increased up to 4.96% under the optimized condition. Ahmed at al. [9] designed an ORC to waste heat recovery from a cement plant with an exhaust gas temperature and mass flow rate of 200 °C and 28 kg/s, respectively, and a kiln fuel consumption of 42 kg/s. It was concluded that the effectiveness of ORC heat exchanger may lead up to 93% if R134a is utilized as working fluid. A multi-objective optimization of using ORC as a bottom cycle of a cement plant to waste heat recovery was studied in [10] considering exergy, exergoeconomic and exergoenvironmental principles. They used three different working fluids in their simulations and carried out a comprehensive parametric study. They selected cyclohexane as the best working fluid from the exergy and economic points of view, while benzene was much preferred considering the environmental aspect. Tan et al. [11] proposed three waste heat recovery options for cement industry, namely dual pressure power generation, post-combustion carbon capture and combination of these techniques. Technical investigation was made from perspectives of power production capacity and CO_2 capture ratio and it was shown that power generation system has the best economic performance. Karellas et al. [12] compared Rankine cycle and ORC energetically and exergetically as the waste heat recovery options from the cement industry. They reported that power generation from waste gas can contribute in the plant power consumption, significantly. Furthermore, it was shown that for the source temperature of higher than 310 °C, steam Rankine cycle could operate more efficient than the ORC operating with isopentane. Wang et al. [13] compared employing Kalina cycle, ORC and single flash and dual pressure steam cycles to harvest waste heat from the clinker cooler exhaust and preheater exhaust gases in cement plant using exergy analysis. In addition, each combined system was optimized using genetic algorithm. It was revealed that the utilized turbine, condenser and vapor generator unit are the most exergy destructive components and generally Kalina cycle performs better than the others considering exergy efficiency as the final target. Chang et al. [14] proposed a residential CCHP system based on the solar energy and proton exchange membrane fuel cell equipped with ORC, domestic hot water and vapor compression cycle. The effects of some decision parameters, i.e., current density and ambient temperature on the system performance were also taken into account in this study. It was shown that the system efficiency increases with current density both in

summer and in winter, reaching 75.4% and 85.0%, respectively. This system was analyzed using energy and exergy principles and considering six different working fluids by Chang et al. [15]. The results showed that the average coefficient of performance (COP) of the CCHP operating with R601 is 1.19 in summer and 1.42 in winter, and the average exergy efficiencies are 46% and 47% under normal operating conditions. In addition, technical performance analysis of the system was studied in [16] and it was revealed that payback period of the system could reduce from 9.6 to 6 years, if there is no solar energy usage.

As the review of the relevant literature showed many aspects of waste heat recovery from cement plants have been thoroughly investigated. However, two main gaps still exist in the body of knowledge. First, CCHP configurations have not been studied in depth as a waste heat recovery option from cement plants. All the reviewed literature mainly considered the electricity generation from such facilities, while the potential of a cogeneration bottoming cycle was relatively unexplored. Second, the vast majority of the studies have considered only thermodynamic aspects of employing steam cycle and ORC and not economic characteristics, making the obtained results difficult to generalize. In the present study two CCHP systems are presented and compared from the thermodynamic, sustainability and economic points of view. ORC and steam cycle are considered as the electricity generating units in the CCHPs. Different working fluids are considered for the ORC and results are reported for the most appropriate one. Within the both power producing blocks, the condenser is considered to be practically a phase change heat exchanger attached to the local district heating system to supply the released heat from the working fluid, while being condensed. Specific exergy costing (SPECO) method is applied to evaluate the exergoeconomic performance of the suggested systems. Moreover, to allow for more general results, thermodynamic and economic performances of the systems are evaluated under different cooling demands.

As a whole, the highlighted contributions of the present study compared to the previous studies in this subject area can be summarized as follows:

- Utilizing a specific waste heat source of a cement plant with real data to run a domestic-scale CCHP system.
- Comparing different CCHP systems established on the steam cycle and ORC thermodynamically and economically.

- Sustainability index is considered as a decisive tool relating exergy analysis and environmental impact to compare the presented system from the sustainable development point of view.

The remainder of this paper is also organized as follows. Section 2 describes the examined system. The governing principles in terms of thermodynamics and exergoeconomics are presented in section 3. section 4 provides the obtained results while Section 5 concludes the paper.

2. Description of the proposed systems and frameworks

A simplified schematic diagram of the Şanliurfa cement plant is illustrated in Fig. 1. A detailed information about this plant as a standalone system can be found in the literature [17,18]. Exhaust gasses exiting the Pyro-processing tower are supposed to be as the candidate waste heat which is shown with stream number of 21 in the figure. Table 1 outlines thermodynamic characteristics of this stream. A noteworthy point about the existence SO_2 in the waste heat source is that there is a flue gas cleaning (or flue gas treatment) step which ensures the pollution of the flue gas reaches to almost zero. For example, wet flue gas cleaning is an efficient way to bring the flue gases down to near zero emission levels in SO_2, HCl and NH_3. As such, a customized flue gas scrubber solution enables capturing particulate emissions too [19].

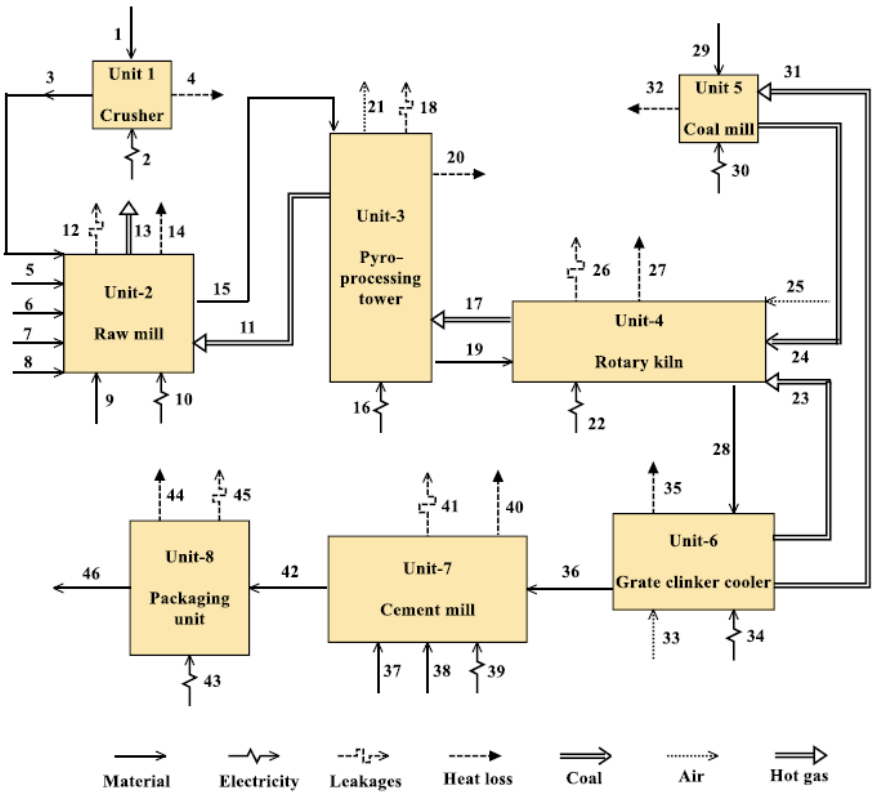

Fig. 1 Schematic diagram of the Şanliurfa cement plant as the considered case study [18]

Table 1

Thermodynamic properties of the selected waste heat source [18]

Stream no. in Fig. 1	Temperature (K)	Mass flow rate (kg/s)	Compositions
21	523	18.43	68.9% N_2, 22.5% CO_2, 5.8% H_2O, 1.1% O_2, 1% Ar, 0.7% SO_2

Figs. 2 and 3 indicate the proposed CCHP systems for waste heat recovery from the mentioned cement plant. In both configurations shown in these figures, the power generation is followed by heating/cooling production. Ideally, this is the most efficient layout from the exergy methodology point of view. The system shown in Fig. 2 is based on the Rankine cycle in which a simple steam cycle is employed to produce power. As the figure shows, waste heat is used first in the heat recovery steam generator (HRSG) to run the Rankine cycle. Produced superheated steam in the HRSG enters the steam turbine (ST) where the enthalpy drop changes into mechanical power. Heat rejection from steam condenser (SC) is utilized for space heating (SPH) purposes. The condensed steam exits the SC in the saturated liquid condition and completes the cycle through pressurizing in the employed pump (SP). HRSG exiting waste gas is warm enough to be utilized in space cooling (SPC) and domestic hot water (HW) production. Then, it is separated into two parts. One is fed to run a single effect LiBr-H_2O absorption chiller to supply domestic space cooling and the next to warm up the pressurized water to deliver domestic hot water via employed heat exchanger (HE). In the chiller subsystem, LiBr (lithium bromide) is considered as the absorbent, while water operates as the refrigerant. A solution of water and LiBr is created in the absorber (Abs), while LiBr absorbs the water refrigerant. Then, this strong solution is pressurized, passed through the solution heat exchanger (SHE) and is finally fed to the generator (Gen). In the generator, the solution is heated and the water content gets vaporized and moves to the condenser (Cond), while the weak solution flows back to the absorber and further absorbs water coming from the evaporator.

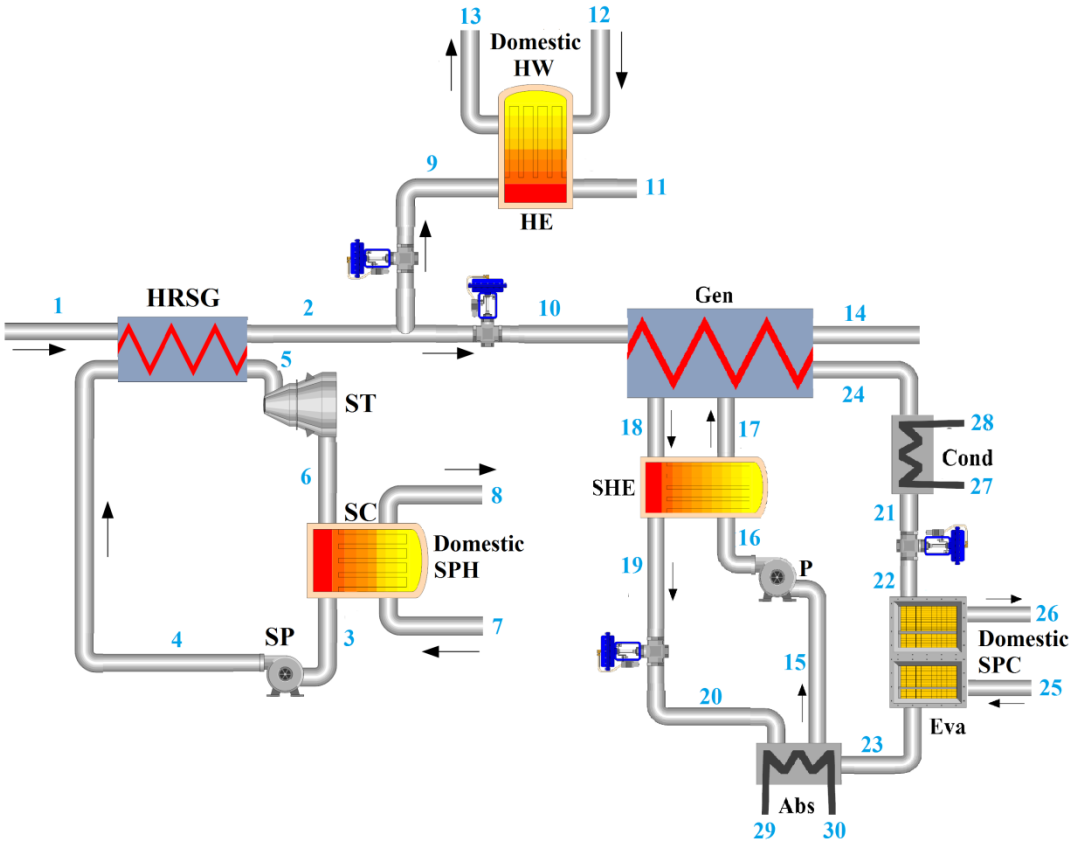

Fig. 2 Schematic diagram of the proposed CCHP system based on the steam cycle

The CCHP system based on the recuperative ORC is shown in Fig. 3. In fact, in this system an ORC is replaced with the steam Rankine cycle. Three refrigerants (R123, R245fa and n-pentane) and two siloxanes (MM and MDM) are utilized as the working fluid in the ORC. Based on the waste heat source temperature and utilization of siloxanes as the working fluid it is decided to use a recuperative ORC rather than a simple ORC [20]. However, it should be highlighted that when the refrigerant is utilized as the working fluid, simple ORC is considered in the CCHP simulation.

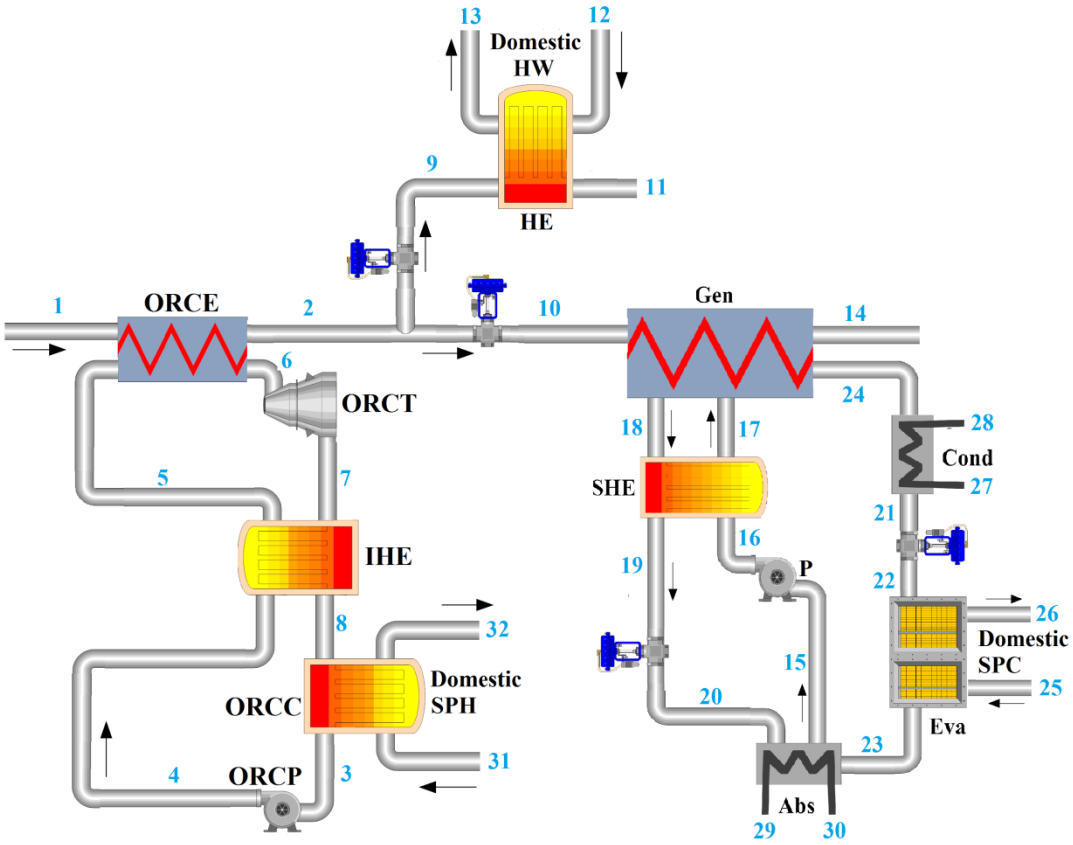

Fig. 3 Schematic diagram of the proposed CCHP system based on the recuperative ORC

In order to simplify the simulation, it was supposed that the whole system operates under steady state condition [21–24] and there was no pressure drop within the components and pipelines [23]. Also, consumed power by the coolant circulatory system in the condensers is ignored [25,26]. Since whole the system operates under the steady state condition, a change in the demand load of the neighborhood doesn't change the system performance. Thus, off-design analysis is not carried out. Although this makes an uncertainty of the simulations compared to the real-life operation of CCHPs, it still might be reasonable for waste heat driven CCHP plants. This is because firstly, such cogeneration plants are mainly employed for base-load coverage and as a result they usually work at full load [27], and secondly, the performance degradation a CCHP system is not a linear function of the operation load and the effects are much less when working on a load above 70-75% of the nominal capacity [28]. In addition, it is hypothesized that the dwelling network has an access to the main grid of heating, cooling and electricity and during high demand periods, the extra possible

demand is fed by the mains. Also, during low demand days, it is possible that the excess heating, cooling or electricity produced by CCHPs to be injected to the main grid.

On the other hand, referring to the climate condition of the case study, the cool season lasts for 3.7 months, from November 24 to March 14, with an average daily high temperature below 15°C , while the maximum value does not exceeds 20°C. Then, the return temperature of the SPH circuit is supposed to be 298 K (5 degree more than the highest ambient temperature during cold days).

Table 2

List of input data and the main framework

Input data	Value	Unit
Steam turbine inlet pressure	2 - 6	bar
Steam turbine inlet superheating degree	20-80	K
Steam turbine outlet quality	> 90	%
Minimal pinch temperature in HRSG	10	K
Steam/ORC turbine isentropic efficiency	90	%
Pumps isentropic efficiency	85	%
Electric generator efficiency [29]	95	%
Coolant water temperature	293	K
DHW supply / return temperature [30]	353 / 313	K
SPH supply / return temperature [31]	313 / 298	K
SPC supply / return temperature [32]	278 / 285	K
Generator temperature	348 - 358	K
Heat exchangers effectiveness	85	%
Minimal pinch temperature in ORCE	10	K
Minimal pinch temperature in Cond	5	K
Portion of the waste gases fed to run the chiller	50	%
Economic value of residual gas from the cement plant [5,18]	0	$/GJ
Ambient temperature	298	K
Ambient pressure	1.013	bar

3. Thermodynamic and exergoeconomic model

3.1. Energy analysis

In order to analyze the proposed system energetically, each component is considered to be a separate control volume. Then, mass balance and energy conservation equations are applied as follows [33]:

$$\sum \dot{m}_i = \sum \dot{m}_o \tag{1}$$

$$\sum \dot{m}_i h_i + \dot{Q} = \sum \dot{m}_o h_o + \dot{W} \tag{2}$$

where, $\dot{m}$, h, $\dot{Q}$ and $\dot{W}$ refer to the mass flow rate, specific enthalpy, rate of heat and mechanical power, respectively, while subscripts i and o denotes inlet and exiting flows, respectively. Governing energy equations for the proposed CCHP systems components are listed in Table 3.

Table 3

The governing energy equations on the components of the proposed CCHP systems

Component	Equation	
HRSG	$\dot{m}_1(h_1 - h_2) = \dot{m}_4(h_5 - h_4)$	(3)
ST	$\dot{W}_{ST} = \dot{m}_5(h_5 - h_6)$, $\eta_{is,ST} = \dfrac{\dot{W}_{ST}}{\dot{W}_{is,ST}}$	(4)
SC	$\dot{m}_6(h_6 - h_3) = \dot{m}_7(h_8 - h_7)$	(5)
SP	$\dot{W}_{SP} = \dot{m}_3(h_4 - h_3)$, $\eta_{is,SP} = \dfrac{\dot{W}_{is,SP}}{\dot{W}_{SP}}$	(6)
ORCE	$\dot{m}_1(h_1 - h_2) = \dot{m}_5(h_6 - h_5)$	(7)
ORCT	$\dot{W}_{ORCT} = \dot{m}_6(h_6 - h_7)$, $\eta_{is,ORCT} = \dfrac{\dot{W}_{ORCT}}{\dot{W}_{is,ORCT}}$	(8)
IHE	$\dot{m}_7(h_7 - h_8) = \dot{m}_4(h_5 - h_4)$	(9)
ORCC	$\dot{m}_8(h_8 - h_3) = \dot{m}_{31}(h_{32} - h_{31})$	(10)
ORCP	$\dot{W}_{ORCP} = \dot{m}_3(h_4 - h_3)$, $\eta_{is,ORCP} = \dfrac{\dot{W}_{is,ORCP}}{\dot{W}_{ORCP}}$	(11)
HE	$\dot{m}_9(h_9 - h_{11}) = \dot{m}_{12}(h_{13} - h_{12})$, $eff_{HE} = \dfrac{Max\{(T_{13} - T_{12}), (T_9 - T_{11})\}}{T_9 - T_{12}}$	(12)
Gen	$\dot{m}_{10}h_{10} + \dot{m}_{17}h_{17} = \dot{m}_{14}h_{14} + \dot{m}_{18}h_{18} + \dot{m}_{24}h_{24}$	(13)
SHE	$\dot{m}_{16}(h_{17} - h_{16}) = \dot{m}_{18}(h_{18} - h_{19})$, $eff_{SHE} = \dfrac{Max\{(T_{17} - T_{16}), (T_{18} - T_{19})\}}{T_{18} - T_{16}}$	(14)
Cond	$\dot{m}_{24}(h_{24} - h_{21}) = \dot{m}_{27}(h_{28} - h_{27})$	(15)
Eva	$\dot{m}_{22}(h_{23} - h_{22}) = \dot{m}_{25}(h_{25} - h_{26})$	(16)

Abs	$\dot{m}_{20}h_{20} + \dot{m}_{23}h_{23} + \dot{m}_{29}h_{29} = \dot{m}_{30}h_{30} + \dot{m}_{15}h_{15}$	(17)
P	$\dot{W}_P = \dot{m}_{15}(h_{16} - h_{15}),\ \eta_{is,P} = \dfrac{\dot{W}_{is,P}}{\dot{W}_P}$	(18)

Since the considered CCHP systems produce electricity, heating and cooling, simultaneously, then energy utilization factor (EUF) is defined to evaluate the systems performances from the first law point of view [34]:

$$EUF = \frac{\dot{W}_{net} + \dot{Q}_{SPH} + \dot{Q}_{DHW} + \dot{Q}_{SPC}}{\dot{m}_1 h_1 - \dot{m}_{11} h_{11} - \dot{m}_{14} h_{14}} \tag{19}$$

in which, $\dot{W}_{net}$, $\dot{Q}_{SPH}$, $\dot{Q}_{DHW}$ and $\dot{Q}_{SPC}$ are the net produced power by the system, rate of delivered heat as space heating, rate of delivered heat as domestic hot water and rate of delivered cooling to be used in domestic air conditioning. Mentioned parameters can be defined as follows:

$$\dot{W}_{net} = \eta_{gen}\dot{W}_{ST/ORCT} - \dot{W}_{SP/ORCP} - \dot{W}_P \tag{20}$$

$$\dot{Q}_{SPH} = \dot{m}_{10}(h_{11} - h_{10}) + \dot{m}_{29}(h_{30} - h_{29}) \tag{21}$$

$$\dot{Q}_{DHW} = \dot{m}_{32}(h_{33} - h_{32}) \tag{22}$$

$$\dot{Q}_{SPC} = \dot{m}_{22}(h_{23} - h_{22}) \tag{23}$$

3.2. Exergy analysis

Exergy is an extensive property of the system and can be defined as the maximum theoretical useful work (shaft work or electrical work) obtainable as the systems interact to equilibrium, heat transfer occurring with the environment only [35]. In the absence of nuclear, magnetic, electrical, and surface tension effects, the total exergy of a system can be divided into physical (a.k.a. thermomechanical) and chemical exergies (potential and kinetic exergies) are ignored [36]:

$$e = e_{ph} + e_{ch} \tag{24}$$

Since changes of the composition do not occur in the proposed CCHP systems, chemical exergy is not considered. Physical exergy of a stream is a function of ambient and the stream conditions and can be written as [37]:

$$e_{ph} = h - h_0 - T_0(s - s_0) \tag{25}$$

Subscript *0* symbolizes ambient dead state condition. Exergy rate in each stream is:

$$\dot{E}_i = \dot{m}_i e_i \tag{26}$$

Unlike the energy, exergy is not conserved and may destroy or loss during a thermodynamic process. However, it is worth mentioning that a part of the exergy destruction is because of component internal irreversibilities, while some can be the exergy loss like discharged exergy to the environment (e.g., coolant) without any usage. Exergy balance equation is applied for each system component as follows:

$$\sum_{in} \dot{E} = \sum_{out} \dot{E} + \dot{E}_D \tag{27}$$

Definition of fuel and product for each component makes it easy to understand the exergy destruction within them. In fact, fuel is the consumed exergy in each unit to generate product in terms of exergy. Table 4 lists the exergy balance equations for the both suggested CCHP systems. Motivated readers are referred to texts i.e., Kotas [38] or Szargut et al. [39] to get more in depth knowledge on exergy principles.

Table 4

Exergy balance equations of the proposed CCHP system components

Component	Fuel	Product	Exergy destruction	
HRSG	$\dot{E}_1 - \dot{E}_2$	$\dot{E}_5 - \dot{E}_4$	$\dot{E}_1 - \dot{E}_2 - (\dot{E}_5 - \dot{E}_4)$	(28)
ST	$\dot{E}_5 - \dot{E}_6$	$\dot{W}_{ST}$	$\dot{E}_5 - \dot{E}_6 - \dot{W}_{ST}$	(29)
SC	$\dot{E}_6 - \dot{E}_3$	$\dot{E}_8 - \dot{E}_7$	$\dot{E}_6 - \dot{E}_3 - (\dot{E}_8 - \dot{E}_7)$	(30)
SP	$\dot{W}_{SP}$	$\dot{E}_4 - \dot{E}_3$	$\dot{W}_{SP} - (\dot{E}_4 - \dot{E}_3)$	(31)
ORCE	$\dot{E}_1 - \dot{E}_2$	$\dot{E}_6 - \dot{E}_5$	$\dot{E}_1 - \dot{E}_2 - (\dot{E}_6 - \dot{E}_5)$	(32)
ORCT	$\dot{E}_6 - \dot{E}_7$	$\dot{W}_{ORCT}$	$\dot{E}_6 - \dot{E}_7 - \dot{W}_{ORCT}$	(33)
IHE	$\dot{E}_7 - \dot{E}_8$	$\dot{E}_5 - \dot{E}_4$	$\dot{E}_7 - \dot{E}_8 - (\dot{E}_5 - \dot{E}_4)$	(34)
ORCC	$\dot{E}_8 - \dot{E}_3$	$\dot{E}_{32} - \dot{E}_{31}$	$\dot{E}_8 - \dot{E}_3 - (\dot{E}_{32} - \dot{E}_{31})$	(35)
ORCP	$\dot{W}_{ORCP}$	$\dot{E}_4 - \dot{E}_3$	$\dot{W}_{ORCP} - (\dot{E}_4 - \dot{E}_3)$	(36)
HE	$\dot{E}_9 - \dot{E}_{11}$	$\dot{E}_{13} - \dot{E}_{12}$	$\dot{E}_9 - \dot{E}_{11} - (\dot{E}_{13} - \dot{E}_{12})$	(37)
Gen	$\dot{E}_{10} - \dot{E}_{14}$	$\dot{E}_{18} + \dot{E}_{24} - \dot{E}_{17}$	$\dot{E}_{10} - \dot{E}_{14} - (\dot{E}_{18} + \dot{E}_{24} - \dot{E}_{17})$	(38)
SHE	$\dot{E}_{18} - \dot{E}_{19}$	$\dot{E}_{17} - \dot{E}_{16}$	$\dot{E}_{18} - \dot{E}_{19} - (\dot{E}_{17} - \dot{E}_{16})$	(39)
Cond	$\dot{E}_{24}$	$\dot{E}_{21}$	$\dot{E}_{24} - \dot{E}_{21}$	(40)

Eva	$\dot{E}_{23}-\dot{E}_{22}$	$\dot{E}_{26}-\dot{E}_{25}$	$\dot{E}_{23}-\dot{E}_{22}-(\dot{E}_{26}-\dot{E}_{25})$	(41)
Abs	$\dot{E}_{23}+\dot{E}_{20}+\dot{E}_{29}$	$\dot{E}_{15}$	$\dot{E}_{23}+\dot{E}_{20}+\dot{E}_{29}-\dot{E}_{15}$	(42)
P	$\dot{W}_{P}$	$\dot{E}_{16}-\dot{E}_{15}$	$\dot{W}_{P}-(\dot{E}_{16}-\dot{E}_{15})$	(43)

Considering the entire CCHP system as a control volume, products of the system in terms of the exergy are the net produced electricity, exergy rates associated with the space heating, domestic hot water and space cooling. Then, the overall exergetic efficiency of the entire system was defined as [40]:

$$\varepsilon=\frac{\dot{W}_{net}+\dot{E}_{SPH}+\dot{E}_{13}-\dot{E}_{12}+\dot{E}_{26}-\dot{E}_{25}}{\dot{E}_{1}} \tag{44}$$

In equation above, $\dot{E}_{SPH}$ is defined as follows:

For the case of Rankine-based CCHP:

$$\dot{\mathrm{E}}_{\mathrm{SPH}}=\dot{E}_{8}-\dot{E}_{7} \tag{45}$$

For the case of ORC-based CCHP:

$$\dot{\mathrm{E}}_{\mathrm{SPH}}=\dot{E}_{32}-\dot{E}_{31} \tag{46}$$

Exergy destruction limitation is of interest from the environmental protection and sustainable development points of view, also. As the sustainability index shows, in each energy converting system lower values of exergy destruction will result in lower fuel consumption and lower environmental impacts accordingly [41–43]. Totally, sustainable development has been defined in different ways, but the most frequently used definition refers to “a development which meets the needs of the present without compromising the ability of future generations to meet their own needs” [44,45].

$$SI=\frac{1}{D_{P}} \tag{47}$$

where,

$$D_{P}=\frac{\dot{E}_{D}}{\dot{E}_{in}} \tag{48}$$

In the equation above, $\dot{E}_{in}$ is the rate of total input exergy to the system.

3.3. Exergoeconomic analysis

To introduce a CCHP system as a bottoming cycle for waste heat recovery from the cement plant, not only the thermodynamic aspects, but also the economic priorities should be considered. Exergoeconomics is in fact the combination of exergy analysis and economic principles to provide the system designer or operator with information not obtainable through conventional exergy analysis and economic evaluations, separately [35]. This technique is developed by Tsatsaronis et al. [46] for the first time. Results obtained from the exergoeconomic analysis are crucial to the design and operation of a cost-effective system.

To calculate the required investment in terms of purchased equipment cost, it is needed to refer to the components cost equations. These equations determine cost of each component in a particular size or capacity. As a matter of fact, these cost equations have been obtained by curve fitting to real cost data as a function of the decision parameters for each component [35]. Cost equations associated with the system components are listed in Table A-1 in the Appendix. It is also notable that, purchased equipment cost should be converted from the reference year to the original year using marshal and swift cost index at various years [35].

Capital investment cost of equipment should be levelized using capital recovery factor (CRF) definition to obtain the cost of each component based on the time unit ($\dot{Z}$) [47]. This is needed in cost balance equation, which will be described later in detail.

$$\dot{Z} = Z \times CRF \times \frac{\varphi}{N \times 3600} \tag{49}$$

$$CRF = \frac{i(1+i)^n}{(1+i)^n - 1} \tag{50}$$

In equations above, Z, φ, N, i and n are equipment cost (are listed in Table A-1), maintenance factor (1.06 [48]), system operating hour per year (7446 [49]), interest rate (4% [50]) and system economic life (20 years [35]), respectively.

After defining the costs per time unit, it is possible to apply the cost balance equation to each system component. The cost balance equation states that the cost rate associated with the product of the system in terms of exergy equals the total rate of expenditures made to generate the product, namely the fuel cost rate and the cost rates associated with the capital investment and operating and maintenance as well. Cost balance equation for the k^{th} component can be written as follows [35,51]:

$$\dot{C}_{q,k} + \sum \dot{C}_{i,k} + \dot{Z}_k = \dot{C}_{w,k} + \sum \dot{C}_{o,k} \quad (51)$$

$$\dot{C}_i = c_i \dot{E}_i \quad (52)$$

here, $\dot{C}$ and c are the cost rate and unit cost of exergy in terms of \$/s and \$/GJ, respectively. Cost balance equations applied for the proposed CCHP system components are outlined in Table 5.

Table 5
Cost balance and auxiliary equations applied to each system component

Component	Cost balance equation	Auxiliary equation	
HRSG	$\dot{C}_1 + \dot{C}_4 + \dot{Z}_{HRSG} = \dot{C}_2 + \dot{C}_5$	$\frac{\dot{C}_1}{\dot{E}_1} = \frac{\dot{C}_2}{\dot{E}_2}$	(53)
ST	$\dot{C}_5 + \dot{Z}_{ST} = \dot{C}_6 + \dot{C}_{\dot{W}_{ST}}$	$\frac{\dot{C}_5}{\dot{E}_5} = \frac{\dot{C}_6}{\dot{E}_6}$	(54)
SC	$\dot{C}_6 + \dot{C}_7 + \dot{Z}_{SC} = \dot{C}_3 + \dot{C}_8$	$\frac{\dot{C}_6}{\dot{E}_6} = \frac{\dot{C}_3}{\dot{E}_3}$	(55)
SP	$\dot{C}_3 + \dot{C}_{\dot{W}_{SP}} + \dot{Z}_{SP} = \dot{C}_4$	-	(56)
ORCE	$\dot{C}_1 + \dot{C}_5 + \dot{Z}_{ORCE} = \dot{C}_2 + \dot{C}_6$	$\frac{\dot{C}_1}{\dot{E}_1} = \frac{\dot{C}_2}{\dot{E}_2}$	(57)
ORCT	$\dot{C}_6 + \dot{Z}_{ORCT} = \dot{C}_7 + \dot{C}_{\dot{W}_{ORCT}}$	$\frac{\dot{C}_6}{\dot{E}_6} = \frac{\dot{C}_7}{\dot{E}_7}$	(58)
IHE	$\dot{C}_7 + \dot{C}_4 + \dot{Z}_{IHE} = \dot{C}_8 + \dot{C}_5$	$\frac{\dot{C}_7}{\dot{E}_7} = \frac{\dot{C}_8}{\dot{E}_8}$	(59)
ORCC	$\dot{C}_8 + \dot{C}_{31} + \dot{Z}_{ORCC} = \dot{C}_3 + \dot{C}_{32}$	$\frac{\dot{C}_8}{\dot{E}_8} = \frac{\dot{C}_3}{\dot{E}_3}$	(60)
ORCP	$\dot{C}_3 + \dot{C}_{\dot{W}_{ORCP}} + \dot{Z}_{ORCP} = \dot{C}_4$	-	(61)
HE	$\dot{C}_9 + \dot{C}_{12} + \dot{Z}_{HE} = \dot{C}_{11} + \dot{C}_{13}$	$\frac{\dot{C}_9}{\dot{E}_9} = \frac{\dot{C}_{11}}{\dot{E}_{11}}$	(62)
Gen	$\dot{C}_{10} + \dot{C}_{17} + \dot{Z}_{Gen} = \dot{C}_{14} + \dot{C}_{18} + \dot{C}_{24}$	$\frac{\dot{C}_{24} - \dot{C}_{17}}{\dot{E}_{24} - \dot{E}_{17}} = \frac{\dot{C}_{18} - \dot{C}_{17}}{\dot{E}_{18} - \dot{E}_{17}}$	(63)
SHE	$\dot{C}_{16} + \dot{C}_{18} + \dot{Z}_{SHE} = \dot{C}_{17} + \dot{C}_{19}$	$\frac{\dot{C}_{18}}{\dot{E}_{18}} = \frac{\dot{C}_{19}}{\dot{E}_{19}}$	(64)
Cond	$\dot{C}_{24} + \dot{C}_{27} + \dot{Z}_{Cond} = \dot{C}_{21} + \dot{C}_{28}$	$\dot{C}_{27} = 0$	(65)
Eva	$\dot{C}_{22} + \dot{C}_{25} + \dot{Z}_{Eva} = \dot{C}_{23} + \dot{C}_{26}$	$\frac{\dot{C}_{22}}{\dot{E}_{22}} = \frac{\dot{C}_{23}}{\dot{E}_{23}}$	(66)
Abs	$\dot{C}_{20} + \dot{C}_{23} + \dot{C}_{29} + \dot{Z}_{Abs} = \dot{C}_{15} + \dot{C}_{30}$	$\frac{\dot{C}_{23} + \dot{C}_{20}}{\dot{E}_{23} + \dot{E}_{20}} = \frac{\dot{C}_{15}}{\dot{E}_{15}}$	(67)

P $\dot{C}_{15} + \dot{C}_{\dot{W}_P} + \dot{Z}_P = \dot{C}_{16}$ - (68)

4. Results and discussion

4.1. Model validation

In order to validate the developed simulation model for the proposed systems, the data reported in the literature is used [23].

The validation is performed for the recuperative ORC as studied in [23], comprehensively. In this study, a recuperative ORC is utilized to produce electricity from a specified geothermal heat source. Exergy destruction within the ORC components is compared under the same conditions, while databases utilized for the working fluid's thermophysical properties in both study were the listed data in the library of the EES. Table 6 outlines this comparison. Referring to this table, a good agreement exist between the results obtained in this study and those reported by the literature [23].

Table 6

Comparison of the results with those of reported in the literature [23] for the case of recuperative ORC.

Component	Exergy destruction reported by the Shokati et al. (kW)	Obtained exergy destruction (kW)
Evaporator	625.5	623
Turbine	762.1	764
Recuperator	135.7	121
Preheater	674.1	674
Pump	21.2	18
Condenser	29.1	30.3

4.2. Operating conditions of the Rankine cycle, ORC and chiller

Before presenting the obtained results, optimum operating conditions of the Rankine cycle corresponding to the optimal turbine pressure and the turbine inlet superheating degree, ORC considering different working fluids and absorption chiller regarding the generator temperature are individually studied and considered in the rest of the analysis. In this section, it is supposed that half of the hot gasses exiting from power producing section is fed to run the chiller and the rest is utilized to warm up the pressurized water in order to supply domestic hot water via the employed heat exchanger.

As Fig. 4 shows, both net produced power and total exergy efficiency of the CCHP system operating with Rankine cycle, take the maximum value with a change in the steam turbine inlet pressure in different pressure levels. In addition, referring to this figure, increasing the turbine inlet superheating degree results in an improvement in the system performance. The limitation, however, for the superheating degree is the considered minimum temperature difference in the HRSG. On the other hand, minimum quality of the 90% in the steam turbine outlet is controlled at different pressure levels and superheating degrees. In addition, as can be seen, there is a difference between the optimal pressure levels corresponding to the maximum output power by the Rankine cycle and the maximum total exergy efficiency of the CCHP. To describe this, it should be highlighted that the turbine outlet energy will be recovered by domestic hot water and cooling production. Therefore, to obtain the maximum total exergy efficiency, maximized power production is not the only effective parameter and the exergy rates associated with the hot and chilled water should be considered. Finally, the optimum pressure associated with the total exergy efficiency and maximum superheating degree is selected as the steam cycle operating condition. Fig. A-1 in the Appendix shows the heat transfer process within the HRSG via a T-Q diagram with the aim of indicating the considered pinch point difference.

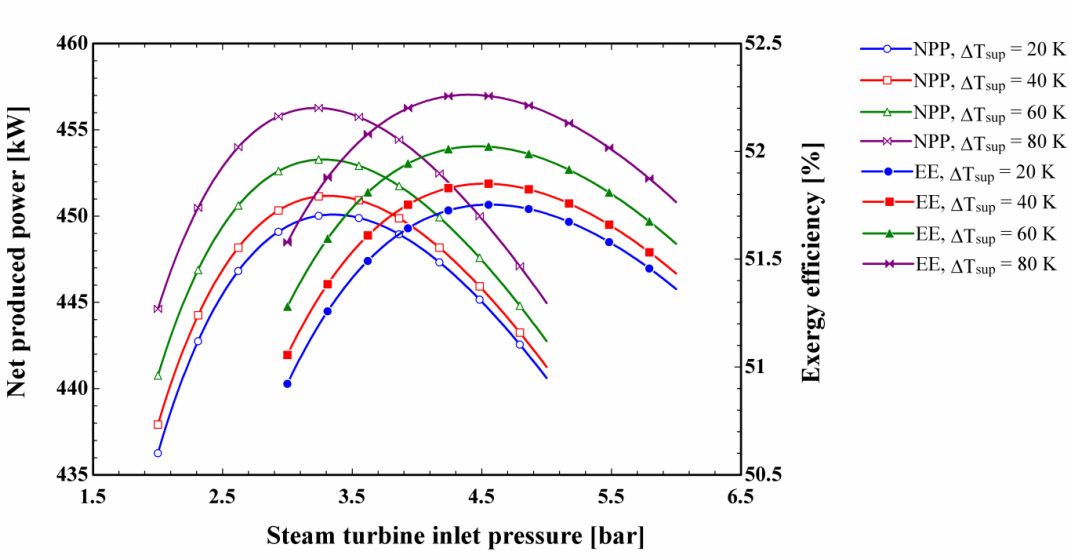

Fig. 4 Net produced power and total exergy efficiency of the steam based CCHP system versus steam turbine inlet pressure and superheating degree

The suitable working fluid in the ORC plays an important role in the ORC-based CCHP system performance. The suitable working fluid must meet both thermodynamic and environmental requirements, i.e., environment-friendly, safety, low ODP (ozone depletion potential), low GWP

(global warming potential) and stable chemical and thermodynamic properties. In designing the ORC it should be mentioned that the maximum pressure in the employed ORC is limited to 95% of working fluid critical pressure. Based on previous studies, supercritical ORC is not a mature technology compared to the subcritical ones. Required multistage pumps with high cost and low efficiency for transcritical ORCs is one of the main reasons why these cycles are not widely adopted [52]. Five different working fluids are utilized in the ORC simulation. Two siloxanes: MM and MDM, three refrigerants: R123, R245fa and n-pentane. Table 7 represents the main characteristics of these working fluids. From the environmental point of view, use of R123 and R245fa is banned by the Montreal protocol and does not pass the EU F-gas Regulation. In addition, R245fa does not pass EC ODS Regulation. However, these refrigerants are utilized as working fluids for ORCs in a wide variety of previous studies [20,25,53,54], and they are employed here for just comparison with siloxanes, which are known as suitable working fluids for high temperature ORCs. More details regarding working fluid selection can be found in the literature [55,56].

Table 7

Thermodynamic properties of the organic working fluids used in the ORC.

Characteristic	MDM	MM	R123	n-pentane	R245fa
Molecular weight (kg/kmol)	236.5	162.4	152.9	72.147	134.05
Critical temperature (˚C)	290.9	245.5	183.7	196.5	154
Critical pressure (bar)	14.15	19.39	36.7	33.64	36.51
Eccentric Factor	0.5301	0.4192	0.2821	0.2499	0.379
Chemical name	Octamethyltris iloxane	Hexamethyldi siloxane	2,2-Dichloro-1,1,1-trifluoroethane	Normal pentane	1,1,1,3,3-Pentafluoropr opane
Chemical formula	C8H24O2Si4	C6H18OSi2	C2HCl2F3	CH3(CH2)3C H3	C3H3F5

Fig. 5 illustrates the net produced power by the ORC and total exergy efficiency of the ORC-based CCHP operating with different working fluids. As can be seen, results associated with MM and MDM are almost the same, while the results related to the refrigerants are not comparable. This is mainly refers to using internal heat exchanger in the high temperature ORCs. Since siloxanes have a higher turbine outlet temperature, it is possible to recover part of the available energy before condensation process. The fact that the siloxanes perform better than the refrigerants for the hypothesized range of source temperature is comprehensively studied in [20], also. However,

among the utilized refrigerants, n-pentane has a better performance, but still lower than siloxnes. Finally, based on the obtained results, MM is selected as the most appropriate working fluid.

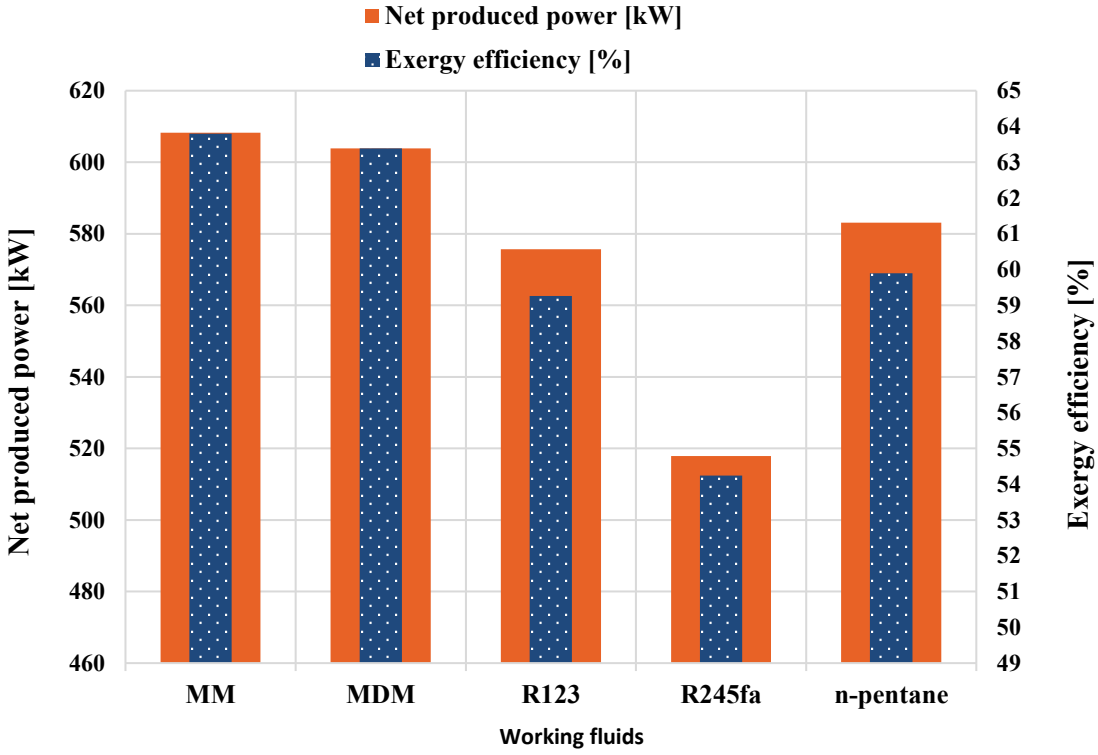

Fig. 5 Effect of using different working fluids in the ORC on the CCHP performance

To evaluate the thermodynamic performance of the employed LiBr-H_2O chiller, generator temperature is the key parameter. As Fig. 6 shows, coefficient of performance (COP) of the chiller hits the maximum value in a generator temperature of approximately 352 K. So, this temperature is chosen as the operating temperature of the examined unit.

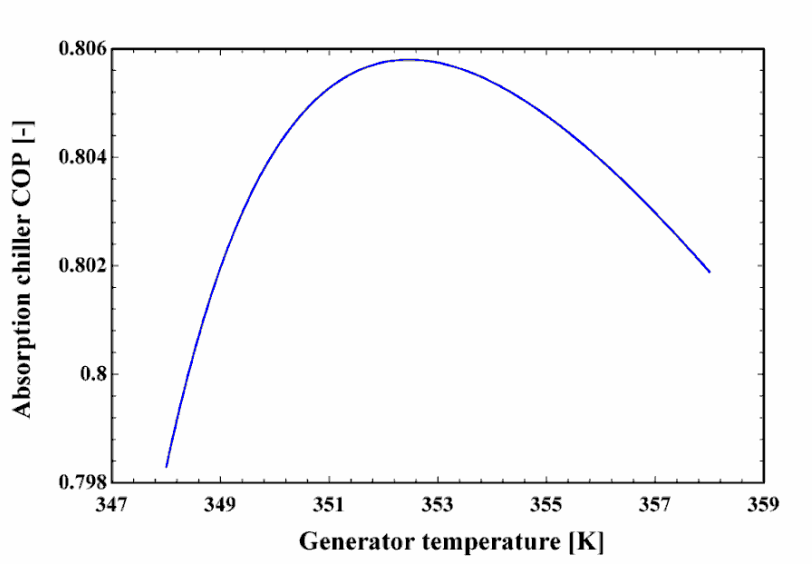

Fig. 6 COP of the absorption chiller versus Gen temperature

4.3. Energy analysis results

The simulation for the proposed systems performance is developed using the Engineering Equation Solver (EES) software [57]. In addition, thermophysical properties of the working fluid are available in the software library. Figs. 7 and 8 illustrate the thermophysical properties of each state in the Rankine- and ORC-based CCHP systems, respectively. Temperature, pressure and mass flow rate are shown in these figures with the units of K, bar and kg/s, respectively. These figures are provided to make it possible to check the thermodynamic principles in different components of the proposed CCHP systems. Obtained optimum operating conditions in the previous section is utilized in the rest of the results.

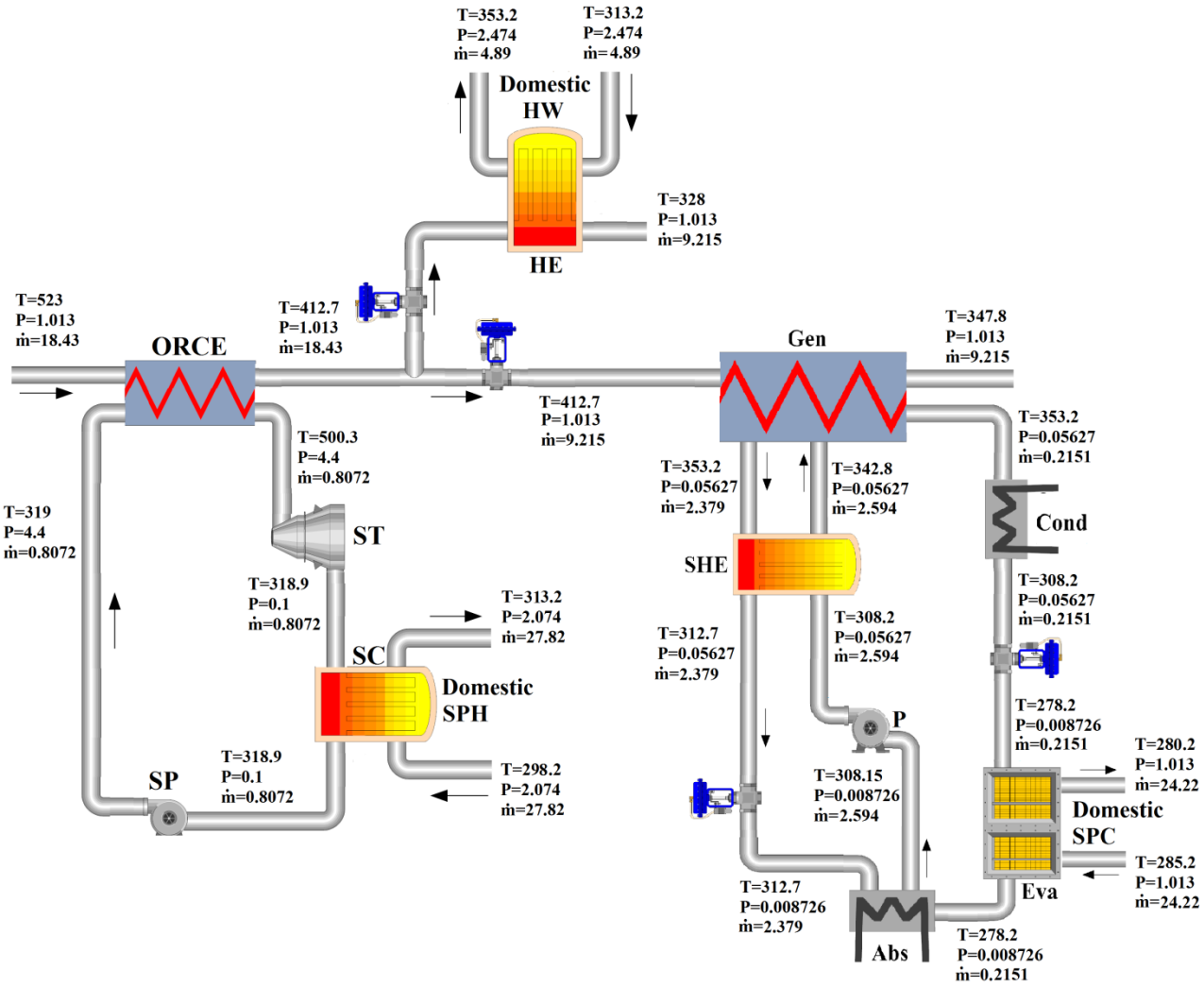

Fig. 7 Thermodynamic properties of each state point of the CCHP operating with Rankine cycle

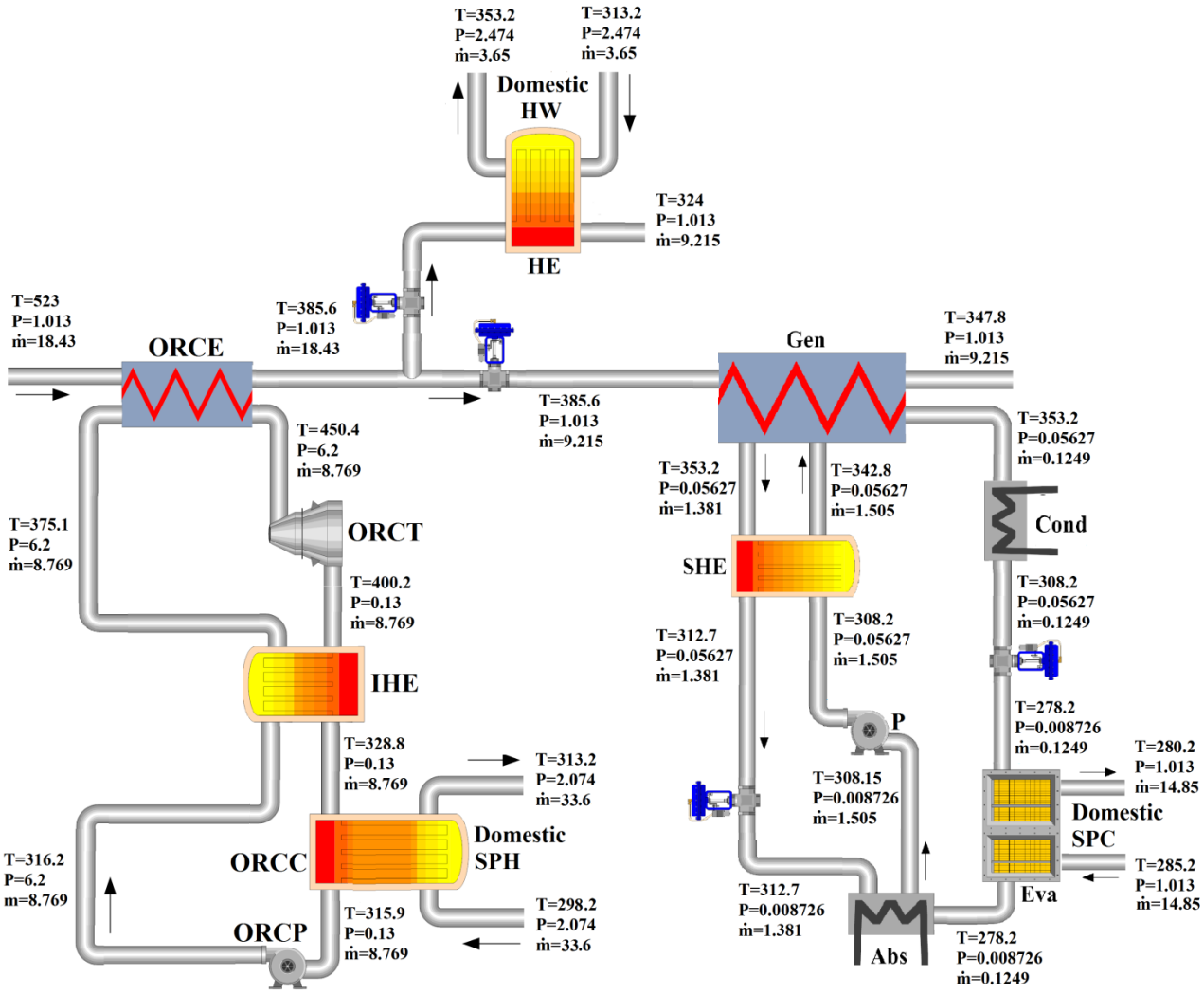

Fig. 8 Thermodynamic properties of each state point of the ORC-based CCHP operating with MM as the working fluid

Table 8 compares the results associated with the energy analysis for the proposed CCHP systems. From the power and domestic space heating generation points of view, ORC-based CCHP system behaves better than the Rankine-based CCHP. In addition, considering the power producing section as a standalone system, ORC shows a better performance with electrical efficiency of 21.97%. However, it should be noted that producing more cooling and domestic hot water is the main characteristic of the CCHP system operating with Rankine cycle. It is worth mentioning that ORC harvests more energy than the Rankine cycle. The ORCE exiting gas has also lower temperature than that of HRSG exiting and this is why the CCHP system based on the Rankine cycle generates more domestic space cooling and hot water. Furthermore, it should be highlighted that the delivered space heating in both systems is completely considerable, 1746 and 2108 kW for the Rankine- and ORC-based systems, respectively, which is harvested from the waste heat of the power producing

sections during the condensation process. Also, mass flow rates of heating and cooling delivering lines in the systems are reported in Table 8, which can be of interest from the heat exchanger design point of view. Referring to this table, working fluid mass flow rate in the ORC is much higher than that of the Rankine cycle that determines turbine size parameter [58] which can be accounted as an important index in the economic aspects of turbomachinery design. Economic results will be reported in the following.

Table 8

Results of the CCHP systems' energy analysis

Parameter	Rankine-based CCHP	ORC-based CCHP
Net produced power [kW]	454.6	593.6
Domestic SPH [kW]	1746	2108
Domestic SPC [kW]	507.3	305.3
Domestic HW [kW]	818.8	605
Working fluid mass flow rate in the power producing unit [kg/s]	0.8072	8.769
Water mass flow rate delivering SPH [kg/s]	27.82	33.6
Water mass flow rate delivering SPC [kg/s]	24.22	14.85
Water mass flow rate delivering domestic HW [kg/s]	4.892	3.65
Power producing section electrical efficiency [%]	20.66	21.97
Absorption chiller COP [-]	0.8057	0.8057
EUF [%]	96.65	98

4.4. Exergy balance

In this section, details of the exergy analysis are reported in terms of destruction and product in each main unit. Fig. 9 shows products of the Rankine-based CCHP in terms of exergy and exergy destruction as well. Referring to this figure, 40% of the total exergy available in the Pyro-processing tower waste gas is converted into electricity, while 28% is destroyed within the Rankine cycle. Because of high value of exergy destruction within this unit, Fig. 10 is represented. As can be seen, HRSG is the main exergy destructive component and 57% of the exergy destruction within the Rankine cycle is due to irreversibilities in this component. T-Q diagram of the HRSG is shown in Fig. A-1. Also, steam condenser causes 28% of steam cycle exergy destruction mainly due to temperature mismatching within this heat exchanger (see Fig. A-2). In total, 40% exergy of the electricity, 8% exergy rate associated with domestic hot water, 3% exergy rate associated with space heating and 2% exergy rate related to space heating show the total exergy efficiency of around 53% for the CCHP system equipped with Rankine cycle.

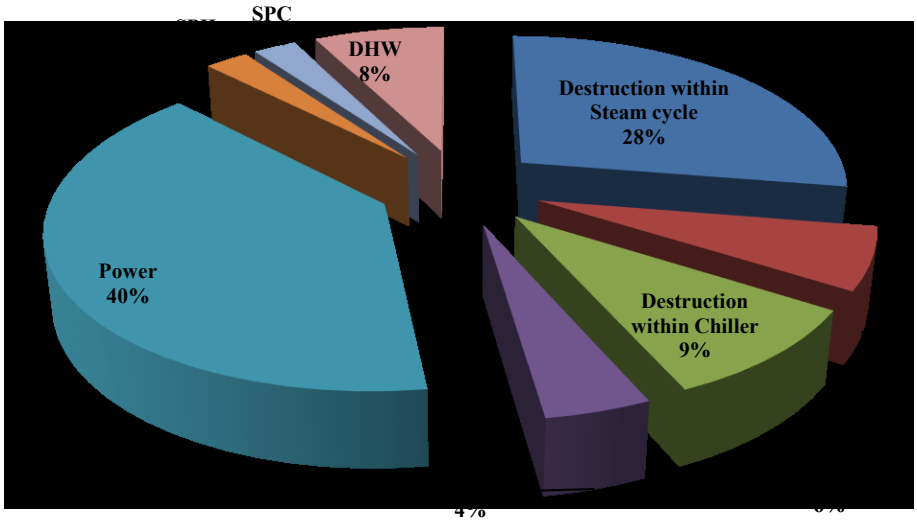

Fig. 9 Exergy balance within the steam-based CCHP

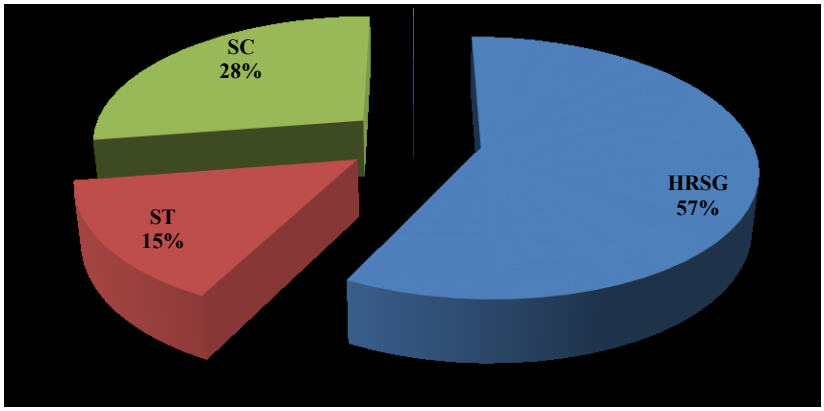

Fig. 10 Share of each component employed in the steam cycle in exergy destruction within this unit

Details of the exergy flow within the ORC-based CCHP system are shown in Fig. 11. As can be seen, ORC recovers more exergy and 54% of the input exergy is converted to the electricity. Moreover, as it was expected, the highest value of exergy destruction belongs to the ORC followed by chiller. Breakdown of the destroyed exergy in the ORC is illustrated in Fig. 12. Based on this figure, 33% of the ORC exergy destruction is due to irreversibilities of the ORCE, thus improving exergetic performance of this component leads to higher exergy efficiency of the whole system. Inappropriate temperature matching is the main reason of exergy destruction in the ORCE and ORCC as well. Figures A-3 and A-4 indicate T-Q diagram of these heat exchangers.

To calculate the total exergy efficiency, sum of the exergy rates associated with electricity, domestic heating, cooling and hot water is considered as the products showing that 63% of the total input exergy is harvested and remain is destroyed or discharged to the atmosphere as the effluent.

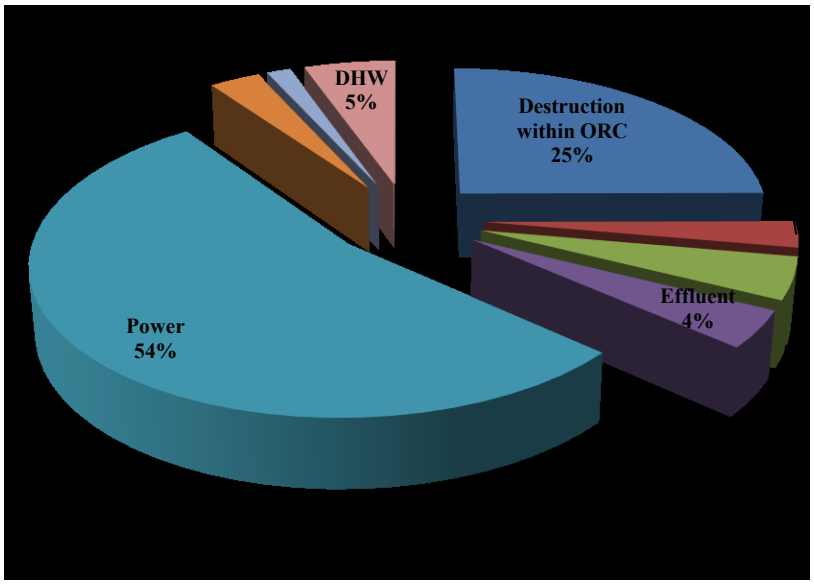

Fig. 11 Exergy balance within the ORC-based CCHP operating with MM as working fluid

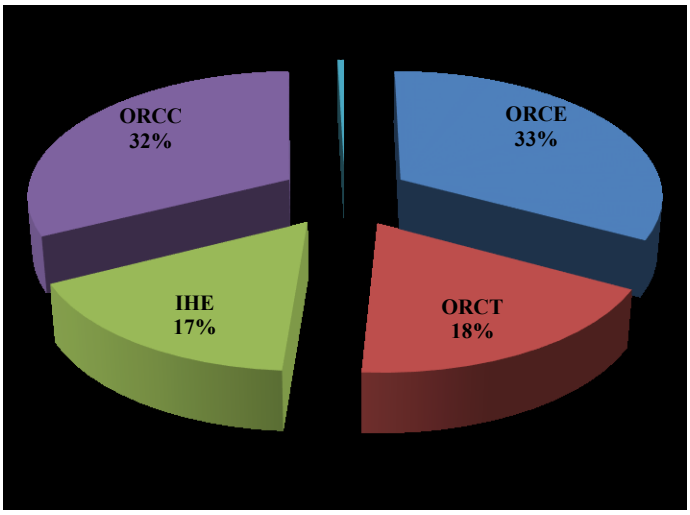

Fig. 12 Share of each component employed in the ORC in exergy destruction within the ORC

It is apparent that the cooling demand (or heating demand) varies during different seasons. Both systems are based on the idea of power generation followed by heating/cooling production. On the other hand, changing cooling demand will change the heating demand, automatically. Therefore, performance of the bottoming CCHPs are evaluated for both summertime and wintertime. As mentioned before, ORC harvests more energy from the waste gases than the Rankine cycle. Thus, hot gases exiting the power producing section in the Rankine-based CCHP has higher temperature and can produce more cooling. Here, it was supposed that space heating demand comes down to zero during the summertime, while takes the maximum value during the wintertime. In addition, It is hypothesized that during summer time required domestic hot water varies from zero to the

maximum amount which can be supplied by the system. In fact maximum cooling capacity means domestic hot water production of zero. Results for both Rankine- and ORC based CCHP are listed in Table 9. As can be seen, during summertime, lower values of cooling production are much favorable from both the first and the second laws of thermodynamics points of view. Decreasing energy utilization factor with increasing cooling demand is mainly due to the chiller COP, which is less than one. In fact, the quantity of the generated cooling by the chiller is less than the utilized heat by this unit. In terms of the exergy, it is worthy of mentioning that the exergy rate associated with domestic hot water is much higher than that of chilled water due to higher temperature difference with ambient condition. Therefore, reduction in the exergy efficiency of the CCHPs with an increase in the cooling demand during the summertime is completely reasonable. Referring to this table, during the summertime, when the cooling demand varies from 0 to 610.7 kW in the ORC-based system energy utilization factor decreases from 46.11to 34.81% and exergy efficiency reduces from 63.51 to 55.36%. For the case of Rankine-based CCHP when cooling demand increases from 0 to 1015 kW energy utilization factor decreases from 54.52 to 42.47% and exergy efficiency reduces from 54.22 to 44.27%.

During the wintertime the energy and exergy rates associated with the space heating demand are taken into account in the energy utilization factor and exergy efficiency, respectively. Also, space cooling of zero and the maximum domestic hot water are considered for wintertime. Therefore, proposed CCHP systems have a better thermodynamic performance during the wintertime.

Table 9

Thermodynamic performance of the proposed CCHPs under the summertime and wintertime conditions

Parameter	Rankine-based CCHP		ORC-based CCHP	
	Summertime	Wintertime	Summertime	Wintertime
Net produced power [kW]	454.6	454.6	593.6	593.6
Domestic SPH [kW]	0	1746	0	2108
Domestic SPC [kW]	0-1015	0	0-610.7	0
Domestic HW [kW]	1638-0	1638	1210-0	1210
EUF [%]	54.52-42.47	100	46.11-34.81	100
Exergy efficiency [%]	54.22-44.27	57.9	63.51-55.36	68.04

4.5. Economic analysis results

Under the base condition, main outcomes from the exergoeconomic analysis are listed in Table 10 and compared for both proposed small-scale CCHP systems. To evaluate the economic incomes of the systems, guaranteed purchased price of electricity, heating and cooling are supposed to be 30, 20 and 20 € per MWh, respectively [50,59]. As the results show, ORC-based CCHP has higher capital investment cost and payback period as well. Therefore, unlike the thermodynamic outcomes, economic results highly recommend the Rankine-based CCHP solution. In fact, higher value of payback period for the case of ORC-based CCHP is due to higher value of capital investment cost and this mainly because of the expander cost. This component is the most expensive part of the ORC and has higher cost rather than a steam turbine. However, unit cost of produced electricity and space heating by the ORC-based CCHP is lower than those of Rankine-based CCHP system.

Table 10

Results of the CCHP systems' economic analysis

Parameter	Steam-based CCHP	ORC-based CCHP
Estimated purchased equipment cost [million $]	0.7	0.78
Estimated total capital investment [million $]	2.9	3.259
Unit cost of produced electricity [$/GJ]	3.268	3.089
Unit cost of produced SPH [$/GJ]	7.858	3.609
Unit cost of produced SPC [$/GJ]	13.29	17.38
Unit cost of produced hot water [$/GJ]	0.6481	1.033
Payback period [year]	4.738	5.074

Fig. 13 illustrates the proposed systems economic behavior and sustainability with a change in the cooling demand. As can be seen, cooling delivery via ORC-based CCHP does not reach 600 kW. For all values of cooling demand, however, the sustainability index of the ORC-based CCHP is higher compared to the Rankine-based CCHP. Then, from the environmental point of view, it is suggested that this system to be chosen as the waste heat recovery solution from Şanliurfa cement plant. This is while, if one considers payback period as a selection criterion, Rankine-based CCHP will be the right choice since this system has lower payback period for all values of cooling demand. Generally, when the chiller unit performs in lower capacity (when domestic hot water production rate is high) both proposed systems have better performance from the viewpoint of thermodynamic, environment and economic. Therefore, the proposed systems behave better during cold seasons. When cooling demand varies from 100 to 500 kW in the ORC-based system sustainability index decreases from 2.964 to 2.551 and payback period increases from 4.677 to 5.469 year. For the case of Rankine-based CCHP when cooling demand increases from 100 to 900

kW sustainability index decreases from 2.24 to 1.906 and payback period increases from 4.112 to 5.293 year.

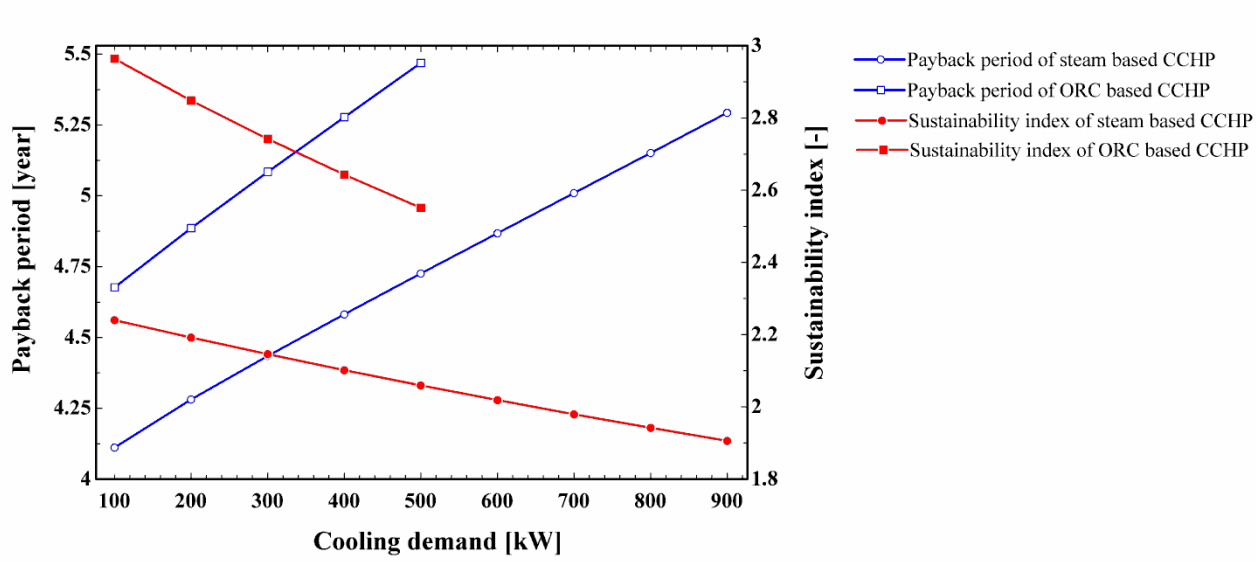

Fig. 13 Proposed CCHP systems' economic and sustainability performance versus cooling demand

5. Conclusion

In the present work two small-scale CCHP systems were proposed to supply domestic electricity, space heating, cooling and hot water demands with the aim of cement plant waste heat recovery. Exhaust gas exiting the Pyro-processing tower from the Şanliurfa cement plant located in Şanliurfa, Turkey is supposed to be as the candidate waste heat and a real data set was utilized. Proposed CCHP systems were based on Rankine and organic Rankine cycles and both of them were equipped with a single effect absorption chiller. In both configurations, the power generation was followed by heating/cooling production. Ideally, this was the most efficient layout from the exergy point of view. The whole idea was an inspiration from the fact that using the available industrial waste heat sources in order to sustainable development is becoming more and more important in the Turkey energy matrix as a developing country. To this end, both configurations were taken as candidate solutions and detailed exergy and exergoeconomic analyses were performed to dig into the very deep thermodynamic, sustainability and economic performance of the proposed systems. Lastly, a sensitivity analysis was carried out to show the effects of changing cooling demand on the system performance. All different sections (steam or organic Rankine cycle and absorption chiller) were optimized individually and MM was selected as the most appropriate working fluid for the ORC.

Under the base condition, the thermodynamic assessments revealed that an exergy efficiency of up to 63% might be achieved from the proposed ORC-based CCHP system when half of the hot gas coming out from power producing section is used to run the chiller. This is while the Rankine-based CCHP operated with 53% of exergy efficiency under the same condition. It was also revealed that 40% of available exergy in the waste heat source could be altered to electricity via steam Rankine cycle, while the recuperative ORC operating with MM converted 54% of input exergy to net electricity. In addition, the main points of irreversibilities in the system were addressed and employed HRSG in the steam cycle and ORCE in the ORC unit found to be the most exergy destructive components. Thermodynamically, it is concluded that the ORC-based CCHP system operating with MM as working fluid has a better performance with energy utilization factor, exergy efficiency and sustainability index of 98.07, 63.6% and 2.747, respectively. This is while, CCHP system based on the Rankine cycle is economically preferable with a payback period of 4.738 year compared to the system operating with ORC and a payback period of 5.074 year.

Acknowledgment

This research is part of the "*HeatReFlex-Green and Flexible District Heating/Cooling*" project (www.heatreflex.et.aau.dk) funded by Danida Fellowship Centre and the Ministry of Foreign Affairs of Denmark to conduct research in growth and transition countries under the grant no. 18-M06-AAU.

Appendix

Table A-1

Cost equation considered for each system component [22,35,48,60–62]

Component	Cost equation	
HRSG	$Z = 6570\left[\left(\frac{\dot{Q}_{eco}}{\Delta T_{LMTD,eco}}\right)^{0.8} + \left(\frac{\dot{Q}_{eva}}{\Delta T_{LMTD,eva}}\right)^{0.8}\right] + 21276\ \dot{m}_s + 1184.4\ \dot{m}_g^{1.2}$	(A-1)
ST	$Z = 3880.5\ \dot{W}_{ST}^{0.7}\left(1+\left(\frac{0.05}{1-\eta_{is,ST}}\right)^3\right)\times\left(1+5\ \exp\left(\frac{T_{in}-866}{10.42}\right)\right)$	(A-2)
SC	$Z = 280.74\ \frac{\dot{Q}_{Cond}}{2.2\ \Delta T_{LMTD,Cond}} + 746\ \dot{m}_{cw}$	(A-3)
SP	$Z = 705.48\ \dot{W}_{SP}^{0.71}\left(1+\frac{0.2}{1-\eta_{is,SP}}\right)$	(A-4)

ORCE	$Z = 130\ (\frac{A_{ORCE}}{0.093})^{0.78}$	(A-5)
ORCT	$Z = 6000\ \dot{W}_{ORCT}^{0.7}$	(A-6)
IHE	$Z = 1.3\ (119 + 310 A_{IHE})$	(A-7)
ORCC	$Z = 280.74\ \frac{\dot{Q}_{ORCC}}{2.2\ \Delta T_{LMTD,ORCC}} + 746\ \dot{m}_{cw}$	(A-8)
ORCP	$Z = 3540\ \dot{W}_{ORCP}^{0.71}$	(A-9)
HE	$Z = 309.14\ A_{HE}^{0.85}$	(A-10)
Gen	$Z = 17500\ (\frac{A_{Gen}}{100})^{0.6}$	(A-11)
SHE	$Z = 309.14\ A_{SHE}^{0.85}$	(A-12)
Cond	$Z = 280.74\ \frac{\dot{Q}_{Cond}}{2.2\ \Delta T_{LMTD,Cond}} + 746\ \dot{m}_{cw}$	(A-13)
Eva	$Z = 16000\ (\frac{A_{Eva}}{100})^{0.6}$	(A-14)
Abs	$Z = 16000\ (\frac{A_{Abs}}{100})^{0.6}$	(A-15)
P	$Z = 2000\ \dot{W}_{P}^{0.65}$	(A-16)

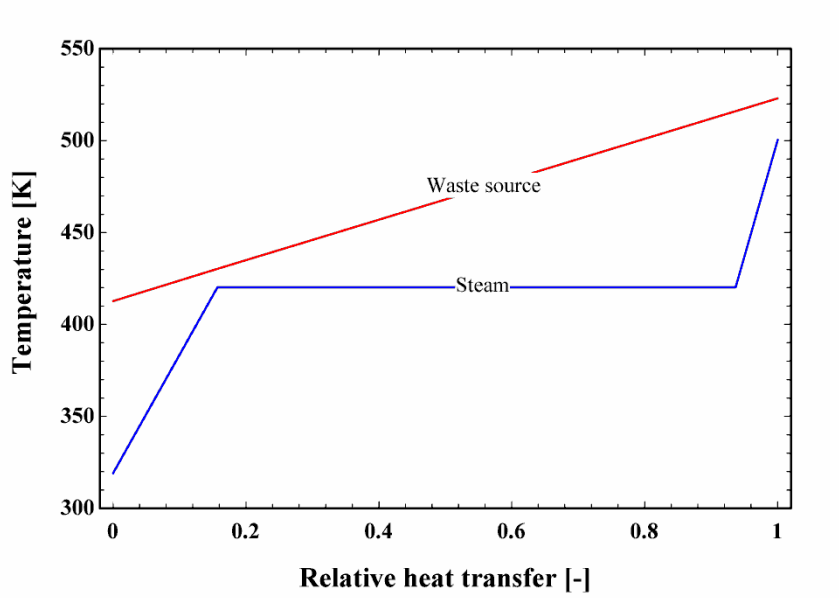

Fig. A-1 T-Q diagram of the HRSG

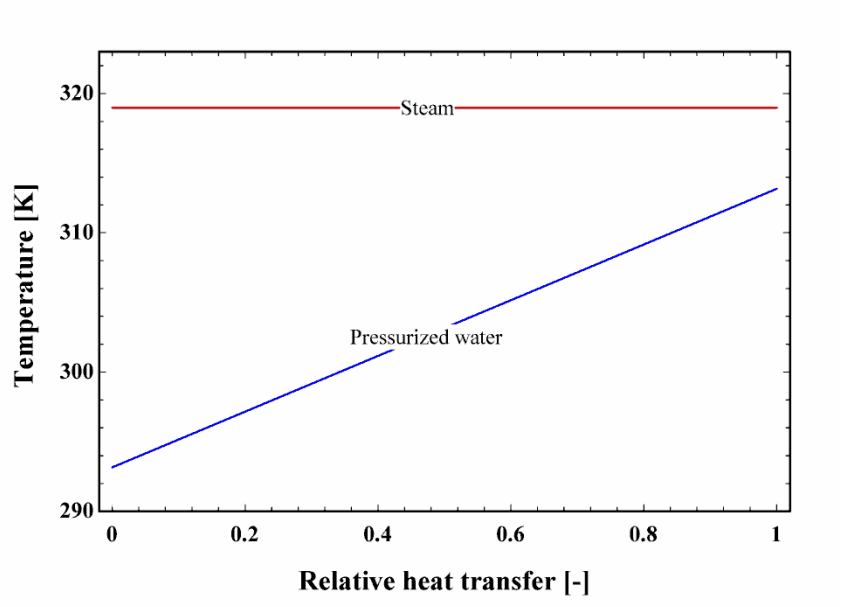

Fig. A-2 T-Q diagram of the SC

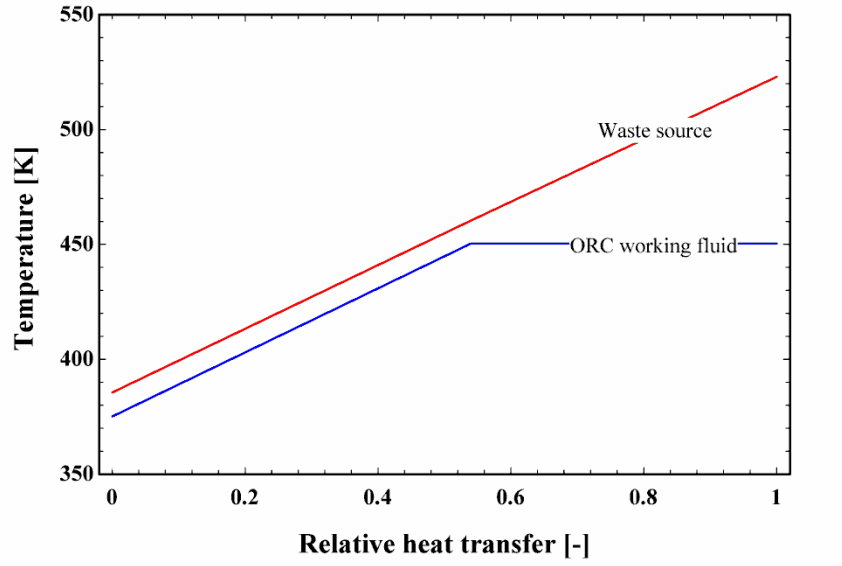

Fig. A-3 T-Q diagram of the ORCE

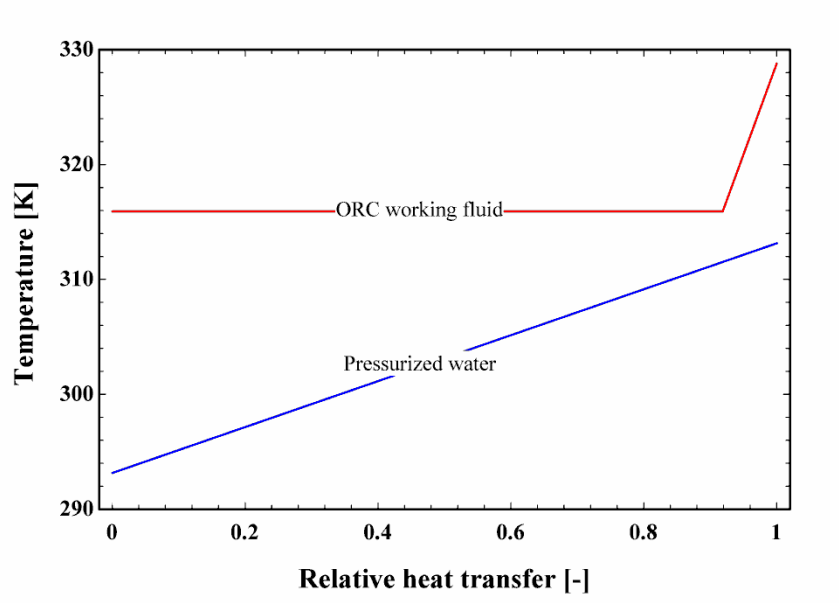

Fig. A-4 T-Q diagram of the ORCC

References

[1] P. KUMAR MEHTA, Greening of the Concrete Industry for Sustainable Development, Concr. Int. 24 (2002) 23–28.

[2] L.B. Kong, T. Li, H.H. Hng, F. Boey, T. Zhang, S. Li, Waste Mechanical Energy Harvesting (I): Piezoelectric Effect, in: Springer, Berlin, Heidelberg, 2014: pp. 19–133. doi:10.1007/978-3-642-54634-1_2.

[3] T. Engin, V. Ari, Energy auditing and recovery for dry type cement rotary kiln systems—A case study, Energy Convers. Manag. 46 (2005) 551–562. doi:10.1016/J.ENCONMAN.2004.04.007.

[4] V. Ghalandari, M.M. Majd, A. Golestanian, Energy audit for pyro-processing unit of a new generation cement plant and feasibility study for recovering waste heat: A case study, Energy. 173 (2019) 833–843. doi:10.1016/J.ENERGY.2019.02.102.

[5] E.P.B. Júnior, M.D.P. Arrieta, F.R.P. Arrieta, C.H.F. Silva, Assessment of a Kalina cycle for waste heat recovery in the cement industry, Appl. Therm. Eng. 147 (2019) 421–437. doi:10.1016/J.APPLTHERMALENG.2018.10.088.

[6] A. Mohammadi, M.A. Ashjari, A. Sadreddini, Exergy analysis and optimisation of waste heat recovery systems for cement plants, Int. J. Sustain. Energy. 37 (2018) 115–133. doi:10.1080/14786451.2016.1181067.

[7] W.S. Amarasinghe, I. Husum, L.-A. Tokheim, Waste heat availability in the raw meal department of a cement plant, Case Stud. Therm. Eng. 11 (2018) 1–14. doi:10.1016/J.CSITE.2017.12.001.

[8] T. Han, C. Wang, C. Zhu, D. Che, Optimization of waste heat recovery power generation system for cement plant by combining pinch and exergy analysis methods, Appl. Therm. Eng. 140 (2018) 334–

340. doi:10.1016/J.APPLTHERMALENG.2018.05.039.

[9] A. Ahmed, K.K. Esmaeil, M.A. Irfan, F.A. Al-Mufadi, Design methodology of organic Rankine cycle for waste heat recovery in cement plants, Appl. Therm. Eng. 129 (2018) 421–430. doi:10.1016/J.APPLTHERMALENG.2017.10.019.

[10] Z. Fergani, D. Touil, T. Morosuk, Multi-criteria exergy based optimization of an Organic Rankine Cycle for waste heat recovery in the cement industry, Energy Convers. Manag. 112 (2016) 81–90. doi:10.1016/J.ENCONMAN.2015.12.083.

[11] Y. Tan, X. Li, L. Zhao, H. Li, J. Yan, Z. Yu, Study on Utilization of Waste Heat in Cement Plant, Energy Procedia. 61 (2014) 455–458. doi:10.1016/J.EGYPRO.2014.11.1147.

[12] S. Karellas, A.-D. Leontaritis, G. Panousis, E. Bellos, E. Kakaras, Energetic and exergetic analysis of waste heat recovery systems in the cement industry, Energy. 58 (2013) 147–156. doi:10.1016/J.ENERGY.2013.03.097.

[13] J. Wang, Y. Dai, L. Gao, Exergy analyses and parametric optimizations for different cogeneration power plants in cement industry, Appl. Energy. 86 (2009) 941–948. doi:10.1016/J.APENERGY.2008.09.001.

[14] H. Chang, Z. Wan, Y. Zheng, X. Chen, S. Shu, Z. Tu, S.H. Chan, Energy analysis of a hybrid PEMFC–solar energy residential micro-CCHP system combined with an organic Rankine cycle and vapor compression cycle, Energy Convers. Manag. 142 (2017) 374–384. doi:10.1016/J.ENCONMAN.2017.03.057.

[15] H. Chang, Z. Wan, Y. Zheng, X. Chen, S. Shu, Z. Tu, S.H. Chan, R. Chen, X. Wang, Energy- and exergy-based working fluid selection and performance analysis of a high-temperature PEMFC-based micro combined cooling heating and power system, Appl. Energy. 204 (2017) 446–458. doi:10.1016/J.APENERGY.2017.07.031.

[16] H. Chang, C. Duan, X. Xu, H. Pei, S. Shu, Z. Tu, Technical performance analysis of a micro-combined cooling, heating and power system based on solar energy and high temperature PEMFC, Int. J. Hydrogen Energy. 44 (2019) 21080–21089. doi:10.1016/J.IJHYDENE.2018.11.217.

[17] A. Atmaca, R. Yumrutaş, Thermodynamic and exergoeconomic analysis of a cement plant: Part I – Methodology, Energy Convers. Manag. 79 (2014) 790–798. doi:10.1016/J.ENCONMAN.2013.11.053.

[18] A. Atmaca, R. Yumrutaş, Thermodynamic and exergoeconomic analysis of a cement plant: Part II – Application, Energy Convers. Manag. 79 (2014) 799–808. doi:10.1016/J.ENCONMAN.2013.11.054.

[19] A. Tabasová, J. Kropáč, V. Kermes, A. Nemet, P. Stehlík, Waste-to-energy technologies: Impact on environment, Energy. 44 (2012) 146–155. doi:10.1016/J.ENERGY.2012.01.014.

[20] H. Nami, I.S. Ertesvåg, R. Agromayor, L. Riboldi, L.O. Nord, Gas turbine exhaust gas heat recovery by organic Rankine cycles (ORC) for offshore combined heat and power applications - Energy and

exergy analysis, Energy. 165 (2018) 1060–1071. doi:10.1016/j.energy.2018.10.034.

[21] V. Zare, A comparative exergoeconomic analysis of different ORC configurations for binary geothermal power plants, Energy Convers. Manag. 105 (2015) 127–138. doi:10.1016/J.ENCONMAN.2015.07.073.

[22] F. Mohammadkhani, N. Shokati, S.M.S. Mahmoudi, M. Yari, M.A. Rosen, Exergoeconomic assessment and parametric study of a Gas Turbine-Modular Helium Reactor combined with two Organic Rankine Cycles, Energy. 65 (2014) 533–543.

[23] N. Shokati, F. Ranjbar, M. Yari, Exergoeconomic analysis and optimization of basic, dual-pressure and dual-fluid ORCs and Kalina geothermal power plants: a comparative study, Renew. Energy. 83 (2015) 527–542.

[24] V. Zare, S.M.S. Mahmoudi, M. Yari, M. Amidpour, Thermoeconomic analysis and optimization of an ammonia--water power/cooling cogeneration cycle, Energy. 47 (2012) 271–283.

[25] M. Yari, Exergetic analysis of various types of geothermal power plants, Renew. Energy. 35 (2010) 112–121. doi:10.1016/j.renene.2009.07.023.

[26] F. Mohammadkhani, F. Ranjbar, M. Yari, A comparative study on the ammonia–water based bottoming power cycles: The exergoeconomic viewpoint, Energy. 87 (2015) 425–434. doi:10.1016/J.ENERGY.2015.05.023.

[27] A. Arabkoohsar, G.B. Andresen, A smart combination of a solar assisted absorption chiller and a power productive gas expansion unit for cogeneration of power and cooling, Renew. Energy. 115 (2018) 489–500. doi:10.1016/J.RENENE.2017.08.069.

[28] T. Savola, I. Keppo, Off-design simulation and mathematical modeling of small-scale CHP plants at part loads, Appl. Therm. Eng. 25 (2005) 1219–1232. doi:https://doi.org/10.1016/j.applthermaleng.2004.08.009.

[29] F. Marty, S. Serra, S. Sochard, J.-M. Reneaume, Simultaneous optimization of the district heating network topology and the Organic Rankine Cycle sizing of a geothermal plant, Energy. 159 (2018) 1060–1074. doi:10.1016/J.ENERGY.2018.05.110.

[30] H. Nami, A. Arabkoohsar, Improving the power share of waste-driven CHP plants via parallelization with a small-scale Rankine cycle, a thermodynamic analysis, Energy. 171 (2019) 27–36. doi:10.1016/j.energy.2018.12.168.

[31] A. Arabkoohsar, Non-uniform temperature district heating system with decentralized heat pumps and standalone storage tanks, Energy. 170 (2019) 931–941. doi:10.1016/J.ENERGY.2018.12.209.

[32] A. Arabkoohsar, G.B. Andresen, Supporting district heating and cooling networks with a bifunctional solar assisted absorption chiller, Energy Convers. Manag. 148 (2017) 184–196. doi:10.1016/J.ENCONMAN.2017.06.004.

[33] Y.A. Cengel, M.A. Boles, Thermodynamics: an engineering approach, 6th ed., McGraw-Hill New

York, 2007.

[34] E. Gholamian, S.M.S. Mahmoudi, V. Zare, Proposal, exergy analysis and optimization of a new biomass-based cogeneration system, Appl. Therm. Eng. 93 (2016) 223–235. doi:10.1016/J.APPLTHERMALENG.2015.09.095.

[35] A. Bejan, G. Tsatsaronis, Thermal design and optimization, John Wiley & Sons, 1996.

[36] Y. Luo, X. Wu, Y. Shi, A.F. Ghoniem, N. Cai, Exergy analysis of an integrated solid oxide electrolysis cell-methanation reactor for renewable energy storage, Appl. Energy. 215 (2018) 371–383. doi:10.1016/j.apenergy.2018.02.022.

[37] A. Lake, B. Rezaie, Energy and exergy efficiencies assessment for a stratified cold thermal energy storage, Appl. Energy. 220 (2018) 605–615. doi:10.1016/j.apenergy.2018.03.145.

[38] T.J. Kotas, The exergy method of thermal plant analysis, 1st ed., Butterworths, London, 1998.

[39] J. Sargut, D.R. Morris, F.R. Steward, Exergy Analysis of Thermal, Chemical, and Metallurgical Processes, Hemisphere Pub, Philadelphia, 1988.

[40] A. Bejan, Advanced engineering thermodynamics, John Wiley & Sons, 2016.

[41] I. Dincer, M.M. Hussain, I. Al-Zaharnah, Energy and exergy use in the industrial sector of Saudi Arabia, Proc. Inst. Mech. Eng. Part A J. Power Energy. 217 (2003) 481–492. doi:10.1243/095765003322407539.

[42] P. Ahmadi, M.A. Rosen, I. Dincer, Multi-objective exergy-based optimization of a polygeneration energy system using an evolutionary algorithm, Energy. 46 (2012) 21–31. doi:10.1016/J.ENERGY.2012.02.005.

[43] P. Ahmadi, M.A. Rosen, I. Dincer, Greenhouse gas emission and exergo-environmental analyses of a trigeneration energy system, Int. J. Greenh. Gas Control. 5 (2011) 1540–1549. doi:10.1016/J.IJGGC.2011.08.011.

[44] I. Dincer, A.S. Joshi, Solar based hydrogen production systems, Springer, 2013.

[45] H. Nami, A. Arabkoohsar, A. Anvari-Moghaddam, Thermodynamic and sustainability analysis of a municipal waste-driven combined cooling, heating and power (CCHP) plant, Energy Convers. Manag. 201 (2019). doi:10.1016/j.enconman.2019.112158.

[46] G. Tsatsaronis, L. Lin, J. Pisa, Exergy Costing in Exergoeconomics, J. Energy Resour. Technol. 115 (1993) 9. doi:10.1115/1.2905974.

[47] A. Nemati, H. Nami, M. Yari, A comparison of refrigerants in a two-stage ejector-expansion transcritical refrigeration cycle based on exergoeconomic and environmental analysis, Int. J. Refrig. 84 (2017) 139–150. doi:10.1016/j.ijrefrig.2017.09.002.

[48] H. Nami, S.M.S. Mahmoudi, A. Nemati, Exergy, economic and environmental impact assessment and optimization of a novel cogeneration system including a gas turbine, a supercritical CO2 and an organic Rankine cycle (GT-HRSG/SCO2), Appl. Therm. Eng. 110 (2017) 1315–1330.

[49] H. Nami, E. Akrami, Analysis of a gas turbine based hybrid system by utilizing energy, exergy and exergoeconomic methodologies for steam, power and hydrogen production, Energy Convers. Manag. 143 (2017) 326–337. doi:10.1016/j.enconman.2017.04.020.

[50] A. Arabkoohsar, H. Nami, Thermodynamic and economic analyses of a hybrid waste-driven CHP–ORC plant with exhaust heat recovery, Energy Convers. Manag. 187 (2019) 512–522. doi:10.1016/j.enconman.2019.03.027.

[51] H. Nami, F. Ranjbar, M. Yari, Methanol synthesis from renewable H2 and captured CO2 from S-Graz cycle – Energy, exergy, exergoeconomic and exergoenvironmental (4E) analysis, Int. J. Hydrogen Energy. 44 (2019) 26128–26147. doi:10.1016/J.IJHYDENE.2019.08.079.

[52] P. Colonna, E. Casati, C. Trapp, T. Mathijssen, J. Larjola, T. Turunen-Saaresti, A. Uusitalo, Organic Rankine Cycle Power Systems: From the Concept to Current Technology, Applications, and an Outlook to the Future, J. Eng. Gas Turbines Power. 137 (2015) 100801. doi:10.1115/1.4029884.

[53] H.D. Madhawa Hettiarachchi, M. Golubovic, W.M. Worek, Y. Ikegami, Optimum design criteria for an Organic Rankine cycle using low-temperature geothermal heat sources, Energy. 32 (2007) 1698–1706. doi:10.1016/j.energy.2007.01.005.

[54] M. Yari, Performance analysis of the different Organic Rankine Cycles (ORCs) using dry fluids, Int. J. Exergy. 6 (2009) 323. doi:10.1504/IJEX.2009.515621.

[55] S. He, H. Chang, X. Zhang, S. Shu, C. Duan, Working fluid selection for an Organic Rankine Cycle utilizing high and low temperature energy of an LNG engine, Appl. Therm. Eng. 90 (2015) 579–589. doi:10.1016/J.APPLTHERMALENG.2015.07.039.

[56] J. Bao, L. Zhao, A review of working fluid and expander selections for organic Rankine cycle, Renew. Sustain. Energy Rev. 24 (2013) 325–342. doi:10.1016/j.rser.2013.03.040.

[57] S.A. Klein, Engineering Equation Solver (EES), fChart Software Inc, Acad. V9. 172 (2012).

[58] A. Nemati, H. Nami, F. Ranjbar, M. Yari, A comparative thermodynamic analysis of ORC and Kalina cycles for waste heat recovery: A case study for CGAM cogeneration system, Case Stud. Therm. Eng. 9 (2017) 1–13. doi:10.1016/j.csite.2016.11.003.

[59] A. Arabkoohsar, M. Dremark-Larsen, R. Lorentzen, G.B. Andresen, Subcooled compressed air energy storage system for coproduction of heat, cooling and electricity, Appl. Energy. 205 (2017) 602–614. doi:10.1016/J.APENERGY.2017.08.006.

[60] S. Soltani, S.M.S. Mahmoudi, M. Yari, T. Morosuk, M.A. Rosen, V. Zare, A comparative exergoeconomic analysis of two biomass and co-firing combined power plants, Energy Convers. Manag. 76 (2013) 83–91. doi:10.1016/J.ENCONMAN.2013.07.030.

[61] E. Akrami, A. Chitsaz, H. Nami, S.M.S. Mahmoudi, Energetic and exergoeconomic assessment of a multi-generation energy system based on indirect use of geothermal energy, Energy. 124 (2017). doi:10.1016/j.energy.2017.02.006.

[62] M. Khaljani, R.K. Saray, K. Bahlouli, Comprehensive analysis of energy, exergy and exergo-economic of cogeneration of heat and power in a combined gas turbine and organic Rankine cycle, Energy Convers. Manag. 97 (2015) 154–165.